Available online at www.sciencedirect.com
ScienceDirect
Precambrian Research 151 (2006) 53–78
Precambrian Research
www.elsevier.com/locate/precamres

Barberton (South Africa) TTG magmas: Geochemical and experimental constraints on source-rock petrology, pressure of formation and tectonic setting

J.D. Clemens [a,*], L.M. Yearron [a], G. Stevens [b]

[a] *School of Earth Sciences and Geography, CEESR, Kingston University, Penrhyn Rd, Kingston-upon-Thames, Surrey KT1 2EE, UK*
[b] *Department of Geology, Stellenbosch University, Matieland 7602, South Africa*

Received 11 August 2004; received in revised form 20 July 2006; accepted 11 August 2006

Abstract

In the southern area of the Barberton Mountain Land, TTG magmas were produced during two distinct, major, magmatic events at ca. 3.44 and 3.23 Ga. Here, as in many Archaean terranes, tonalite-trondhjemite-granodiorite (TTG) plutons are closely associated with basaltic to komatiitic greenstones, in this case with some metamorphosed to amphibolite facies, suggesting a possible genetic connection between the two rock groups. Previous partial melting experiments on metabasic rocks have shown that tonalitic to trondhjemitic melts can be produced, coexisting with amphibole- and plagioclase-rich restites, at pressures of 0.8–1.5 GPa, and garnet- and pyroxene-rich restites at $P \geq 1.5$ GPa. The present experiments on a Barberton greenstone amphibolite confirm the higher pressure findings, except that some amphibole was probably still present. In the case of the 3.23 Ga plutons, the inferred geotherm is consistent with that obtained from metamorphic assemblages of this age from within the Theespruit Formation of the Onverwacht Group. The commonly scattered major- and trace-element variations in the Barberton TTG suite imply that magmatic crystal fractionation played a subordinate role in producing the geochemical variations of the magmas. The different TTG plutons probably represent separate magma batches, and the scattered trends within the plutons probably reflect heterogeneities within their source-rocks. The εNd values suggest that the TTGs were derived from juvenile crustal sources with depleted-mantle signatures. Thus, metabasaltic rocks are the likely sources of the TTG magmas. However, our partial melting experiments on a typical Lower Onverwacht greenstone amphibolite appear to rule out these particular rocks as sources of the local TTG magmas. Instead, it seems likely that possibly more ancient, less potassic, high-grade, metabasic rocks were the sources of the TTG magmas. Trace-element modelling shows that the TTG suite could have been derived through partial melting of primitive basaltic sources, producing plagioclase-free, hornblende-bearing granulitic to eclogitic restites with >30% garnet. Experiments on garnet stability in the near-liquidus mineral assemblage of a typical 3.44 Ga Barberton trondhjemite constrain magma generation to a pressure of at least 1.47 GPa. This suggests that the Barberton crust was relatively cool and at least 50 km thick by 3.44 Ga. The same general argument of high-P melting would hold for the ca. 3.2 Ga trondhjemites and tonalities, although the minimum P of melting has not been determined for these rocks. In the case of these rocks, believed to have formed in response to a major terrane accretion event, the high-P–moderate-T signature is also indicated by recent metamorphic studies. In contrast, information is scarce on the processes operating during the 3.44 Ga magmato-metamorphic event. The P–T conditions during the 3.44 Ga event imply an apparent geothermal gradient of <20 °C/km. The transport of fertile, hydrated metabasic material to such depths suggests that both the 3.23 and 3.44 Ga magmatic events resulted from significant and rapid crustal thickening. This, in turn, suggests that compressional tectonics operated in the Barberton greenstone belt prior to 3.44 Ga.

Keywords: Barberton; Granite; TTG; Archaean; Crustal thickening

* Corresponding author. Fax: +44 20 8547 7497.
E-mail addresses: j.clemens@kingston.ac.uk (J.D. Clemens), l_yearron@hotmail.com (L.M. Yearron), gs@sun.ac.za (G. Stevens).

0301-9268/$ – see front matter © 2006 Elsevier B.V. All rights reserved.
doi:10.1016/j.precamres.2006.08.001

1. Introduction

Tonalite-trondhjemite-granodiorite rocks typically form about two-thirds of the presently accessible Archaean crust (Jahn et al., 1984). The onset of this magmatism is generally believed to represent the transition from dominantly mafic crust, to crust with a significant felsic component (Glikson, 1979). Crustal stabilisation and cratonisation are believed to have developed in short, intense episodes of continental growth, involving magmatic accretion (e.g. Wells, 1981) as well as tectonic thickening and high-grade metamorphism (e.g. De Wit, 1998). As a result, the TTG rocks form an essential element in the 'protocontinental' stage of crustal evolution (Barker, 1979).

The origin of tonalite-trondhjemite magmas has been widely debated. Various suggestions have included fractional crystallisation of basaltic melts (e.g. Arth et al., 1978), partial melting of mantle rocks (e.g. Moorbath, 1975), and the partial melting of pre-existing tonalites (e.g. Johnston and Wyllie, 1988). However, the most widely accepted mechanism for the origin of TTG magmas is by partial melting of hydrous metabasaltic rocks, i.e. greenstones, amphibolites and eclogites, under a variety of fluid conditions and in a variety of tectonic settings (e.g. Martin, 1987; Winther, 1996; Condie, 2005). This latter category of petrogenetic models is largely based on the fact that the chondrite-normalised REE patterns of TTG rocks are typically HREE-depleted and LREE-enriched. Since garnet readily accommodates HREEs, its presence in the crystalline residuum may well account for the HREE-depleted pattern (e.g. Jahn et al., 1981; Rapp et al., 1991; Springer and Seck, 1997). Within this group of models, the main competition is between those that involve fluid-present (but usually highly H_2O-deficient) melting of altered mafic rocks in the downgoing slab (e.g. Prouteau et al., 1999) and those advocating higher-temperature, fluid-absent melting of similar materials, mainly in the deep thickened crust, in a variety of tectonic settings (e.g. Rapp et al., 2003). Foley et al. (2002) presented geochemical evidence that melts with some trace-element ratios similar to those of TTG rocks can be produced by partial melting of low-Mg garnet amphibolites, but not by partial melting of eclogites. They concluded that this melting must have taken place in subduction zones. However, with this model, there are residual difficulties in reproducing some important trace-element characteristics of TTGs (e.g. their Sr, U and Th concentrations). Whatever the source (garnet amphibolite or eclogite), the high pressures necessary to generate TTG melts could still be produced in settings other than subduction zones (e.g. post-subduction collisional thickening of oceanic or arc crust). There are also some difficulties in explaining how subducting slabs retain the required high H_2O contents to the depths necessary for melting and how wet slab melts can ascend through the mantle wedge without being consumed by reactions with the peridotite (see, e.g. Rapp et al., 1999; Prouteau et al., 2001). The fluid-present experiments of Prouteau et al. (1999), on a dacite with TTG-like geochemistry, showed that plagioclase fractionation could only be avoided for melt H_2O contents of 10 wt% or more. This work also showed that the necessary garnet could not have been present near the liquidus of such a magma, at near-source P, T and these fluid conditions. Fluid-absent melting was rejected because such melts, formed at $T \leq 900\,^{\circ}C$, would be too silicic and potassic, and their interaction with the mantle wedge would not alter these parameters significantly. However, the chemistry of the fluid-absent partial melts would depend strongly on the composition of the protolith (Moyen and Stevens, 2005). Also, this neglects the possibility that the slab might not be the setting for TTG genesis and that melting could be at much higher T. The experiments of Rapp et al. (1999) are also instructive. These showed that, with melt:mantle peridotite ratios around 2, slab-derived melts would survive reaction with the mantle. However, for ratios near 1, the melts would be entirely consumed by reaction with the peridotite. Adakites (supposed modern slab melts) have MgO contents and Mg#s that suggest interaction with the rocks of the mantle wedge. However, TTGs have lower MgO and Mg#s than adakitic rocks, and adakitic intrusive rocks do occur in settings unrelated to subduction (e.g. Xu et al., 2002). This suggests that TTG magmas may not have interacted with mantle rocks, and that therefore they were generated in settings in which the magmas could reach emplacement levels without travelling through the mantle (i.e. not by slab melting). Martin and Moyen (2002) and Martin et al. (2005) showed that TTGs generally have higher Mg# than experimentally produced partial melts of basaltic rocks. They also point out that Mg# in parental TTG magmas increased over the Archaean, from 4.0 to 2.5 Ga, suggesting that the degree of interaction between felsic melts and mantle peridotite increased over time. Smithies (2000) showed that such interaction must have been very weak or even absent in TTG magmas older than 3 Ga, and in around 50% of the post-3 Ga TTG magmas as well. Using a similar dataset, Martin et al. (2005) concluded that mantle wedge was either thin or non-existent before 3.4 Ga but that there was a general steepening of subduction angle (and thickening of the mantle wedge) at later times. Despite the volume of work carried out on the problem, the precise nature of the melting reactions

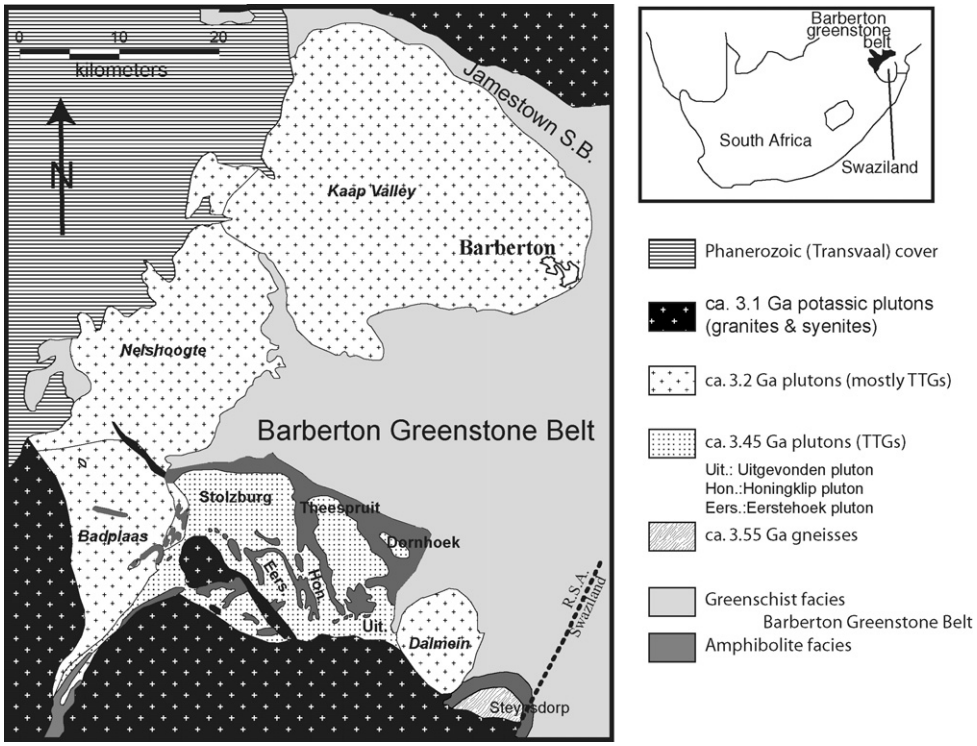

Fig. 1. Summary of the geology of the southern Barberton region.

that produced TTG magmas, and the tectonic settings in which this occurred, remain matters of debate.

Most granitic magmas, including the TTGs, were initially markedly H_2O-undersaturated (e.g. Clemens, 1984; Scaillet et al., 1998; Prouteau et al., 1999). Clemens and Watkins (2001) showed that the observed systematic negative correlation between initial magma temperature and melt H_2O content is consistent only with the magmas being derived through fluid-absent partial melting of pre-existing, hydrous crustal rocks (either deep in the crust or in the upper mantle). Melts with tonalitic and trondhjemitic major-element compositions have been produced by the fluid-absent partial melting of metabasaltic rocks under a wide variety of conditions. Clemens (2005) provides a review of all this experimental work. Rapp et al. (1991) presented a fairly comprehensive study in which they partially melted four natural olivine-normative amphibolites in the pressure range of 0.8–3.2 GPa, at temperatures between 900 and 1150 °C. Results showed that tonalitic to trondhjemitic melts were produced, coexisting with amphibole- and plagioclase-rich restites, at pressures of 0.8 GPa, and garnet- and pyroxene-rich restites at pressures ≥1.6 GPa.

In the Barberton Mountain Land, as in many Archaean terrains, the TTG plutons are closely associated with basaltic to komatiitic greenstones. The Barberton TTG plutons and the highest-grade, amphibolite-facies greenstone rocks are juxtaposed against each other (Fig. 1), and there are many greenstone remnants within the TTG plutons. As a result, a number of South African geologists have concluded that the greenstone rocks represent the source of the TTG magmas (e.g. Robb and Anhaeusser, 1983; Robb, 1983). In this paper we investigate the Barberton TTG rocks, using geochemical and experimental approaches, to address the nature of the protolith and the conditions of TTG magma genesis.

2. Geological setting of TTG magmatism associated with the Barberton greenstone belt

The Palaeo- to Meso-archaean Barberton greenstone belt consists of a well-preserved, early Archaean (3.5–3.2 Ga) volcano-sedimentary succession, comprised of three major lithostratigraphic units. From the base upward, these are:

(1) The 3.50–3.30 Ga Onverwacht Group, composed largely of mafic and ultramafic volcanic rocks, with minor units of felsic volcanic and volcaniclastic rocks, as well as sediments.

(2) The 3.26–3.22 Ga predominantly argillaceous Fig Tree Group, comprised of a succession of greywackes, cherts and shales, plus some dacitic lavas and fragmental volcanic rocks.
(3) The ~3.2 Ga arenaceous sedimentary Moodies Group, which consists largely of feldspathic and quartzose sandstones, polymictic conglomerates, lesser siltstones and shales, and thin units of basalt, jaspilite and magnetite-bearing shale.

This volcano-sedimentary sequence was intruded by two main suites of granitoid magmas between ca. 3.50 and 3.10 Ga. The resulting Barberton granitoid-greenstone terrane was assembled during several tectonomagmatic episodes between ~3.5 and 3.1 Ga (e.g. Anhaeusser and Robb, 1983; Robb and Anhaeusser, 1983; Armstrong et al., 1990; Kamo and Davis, 1994; de Ronde and De Wit, 1994). Early ~3.5 to 3.2 Ga plutonic suites are characterized by tonalites, trondhjemites and granodiorites. The trondhjemites and granodiorites are dominated by sodic plagioclase and quartz with biotite as the major mafic mineral. The tonalites are similar but hornblende is present in addition to biotite and can even dominate the mafic mineral assemblage. In all these rocks, the plagioclase crystals are euhedral to subhedral and were evidently the first felsic phase to crystallise, with the biotite and/or hornblende appearing later in the crystallisation sequence. The composite and commonly internally heterogeneous plutons commonly possess internal contact relationships between magmatic fractions. The plutons are relatively small (<100 to ~500 km^2) and have largely concordant contacts with the greenstones. Some of the felsic rocks are gneissose, particularly near their margins. These structural features have been explained through either the diapiric ascent and emplacement of the TTGs (e.g. Viljoen and Viljoen, 1969; Anhaeusser and Robb, 1983), the synkinematic, shallow crustal underplating of the TTG suite at the base of the largely allochthonous and thrusted greenstone sequences (e.g. De Wit et al., 1987; Armstrong et al., 1990) or as structurally reworked basement, commonly with tectonic rather than intrusive contacts between the greenstones and the TTGs (e.g. Dziggel et al., 2002; Kisters et al., 2003). The TTG rocks themselves generally contain very few mafic magmatic inclusions (enclaves), and the plagioclase feldspars do not show textural evidence of resorbtion. These features suggest that magma mixing and mingling played little part in the production of the TTG magmas, at least at emplacement level.

Collectively, zircon geochronology from several studies (Kamo and Davis, 1994; de Ronde and Kamo, 2000; Armstrong et al., 1990; Kröner et al., 1996, 1991) has demonstrated that there are three clear magmatic age clusters within the TTG suite; the 3509 ± 8 Ma Steynsdorp pluton; the 3460 ± 5 to 3443 ± 4 Ma Stolzburg, Theespruit and Doornhoek plutons; and the 3236 ± 1 to 3227 ± 1 Kaap Valley and Nelshoogte plutons. The age of the youngest Kaap Valley–Nelshoogte TTG generation coincides with the proposed age for the major terrane accretion episode that assembled the rocks of the greenstone belt (Kamo and Davis, 1994; de Ronde and Kamo, 2000). The age of intrusion of these magmas also coincides with the age of peak high-pressure, amphibolite-facies metamorphism, documented from greenstone remnants within the ~3450 Ma TTG intrusions (Dziggel et al., 2002) and within the Theespruit Formation of the greenstone belt (Kisters et al., 2003). Thus, the TTG bodies have been subject to amphibolite-facies metamorphic conditions, and the hornblende compositions and zoning in the plagioclase may have been slightly affected in the older TTG generations. However, since the igneous mineral assemblages are similar to those stable in the upper amphibolite facies, there has been little effect of the metamorphism on the mineralogy or chemistry of the rocks. The metamorphism caused neither dehydration nor partial melting in the TTG rocks, and was essentially isochemical.

The tectonic setting and associations of the older generations of TTGs is more difficult to constrain, principally because of the younger, high-grade metamorphic overprint on these plutonic rocks and the metamafic xenoliths that they include. In several areas within the ~3450 Ma TTG suite, intrusion breccias indicate that these plutons formed as high-level bodies. This is supported by zircon ages, from some of the felsic volcaniclastic components of the Onverwacht Group, that are identical to the crystallization ages of the Theespruit pluton (Armstrong et al., 1990). In places, the plutons cut across the lithological layering of amphibolite facies rocks, indicating their possible association with an older, high-grade metamorphism. However, the details of this metamorphism, as well as its timing relative to the intrusion, are yet to be investigated in detail.

The end of TTG magmatism in the southern Barberton granite-greenstone terrane is marked by the intrusion of the post-tectonic, granodioritic Dalmein pluton at 3216 ± 2 Ma (Kamo and Davis, 1994). This also marks the first appearance of the more potassic granodiorite-monzogranite-syenite suite that is dominated by voluminous plutonism dated at 3107 Ma.

3. Geochemistry

3.1. Methods

Fresh, unaltered rock samples collected during fieldwork were crushed and powdered using a jaw crusher, roller mill and Tema mill. Major- and trace-element data were obtained by X-ray fluorescence spectroscopy (XRF), using a Philips 1404 spectrometer, at the University of Stellenbosch. The spectrometer is fitted with a Rh tube and six analyzing crystals of LIF200, LIF220, LIF420, PE, TLAP and PX1. The detectors used a gas-flow proportional counter and a scintillation detector. The gas-flow proportional counter uses P10 gas. Major elements were analysed on fused glass beads at 50 kV and 50 mA, and trace elements were analysed on pressed powder pellets at 60 kV and 40 mA. Matrix effects were corrected for by applying theoretical alpha factors and measured line overlap factors to the raw intensities, with the SuperQ Philips software. Standards used in the calibration were: AGV-1, BHVO-1, JG-1, JB-1, GSP-1, SY-2, SY-3, STM-1, NIM-G, NIM-S, NIM-N, NIM-P, NIM-D, BCR, GA, GH, DRN and BR. At this facility, standard material AGV-1 is also routinely analysed as a sample, to check for analytical error. Major elements are typically within 1 rel.% of the standard values for elements present at >10 wt%, within 2% for elements present at concentrations between 1 and 10 wt%, and within 7% for elements present at <1 wt%. Measured values for trace elements on AGV-1 were mostly within 10% (usually 5%) of the accepted values, with the exception of Y (20%). Cr and Ni values were affected by contamination from the Tema mill vessels used in sample grinding, so results for these elements are omitted from the data set.

Rare-earth-element data were obtained by inductively coupled plasma atomic emission spectroscopy (ICP-AES) at the University of Stellenbosch and by inductively coupled plasma mass spectroscopy (ICP-MS) in the NERC Facility at Kingston University, UK.

Most mineral and glass (quenched melt) analyses (in the experimental run products to be described later) were carried out on the JEOL 3200 SEM, fitted with an Oxford Instruments ISIS EDS system, at Kingston University. In the products of the TTG near-liquidus experiments, glass areas were sufficiently large that good-quality analyses could be obtained by rastering the beam over large patches of glass, to minimize counting losses on Na. However, in the products of the partial melting experiments on greenstone amphibolite, glass areas were much smaller. To obtain analyses essentially free from Na counting losses, we used a LEO 140VP scanning electron microscope coupled to a Link ISIS energy dispersive

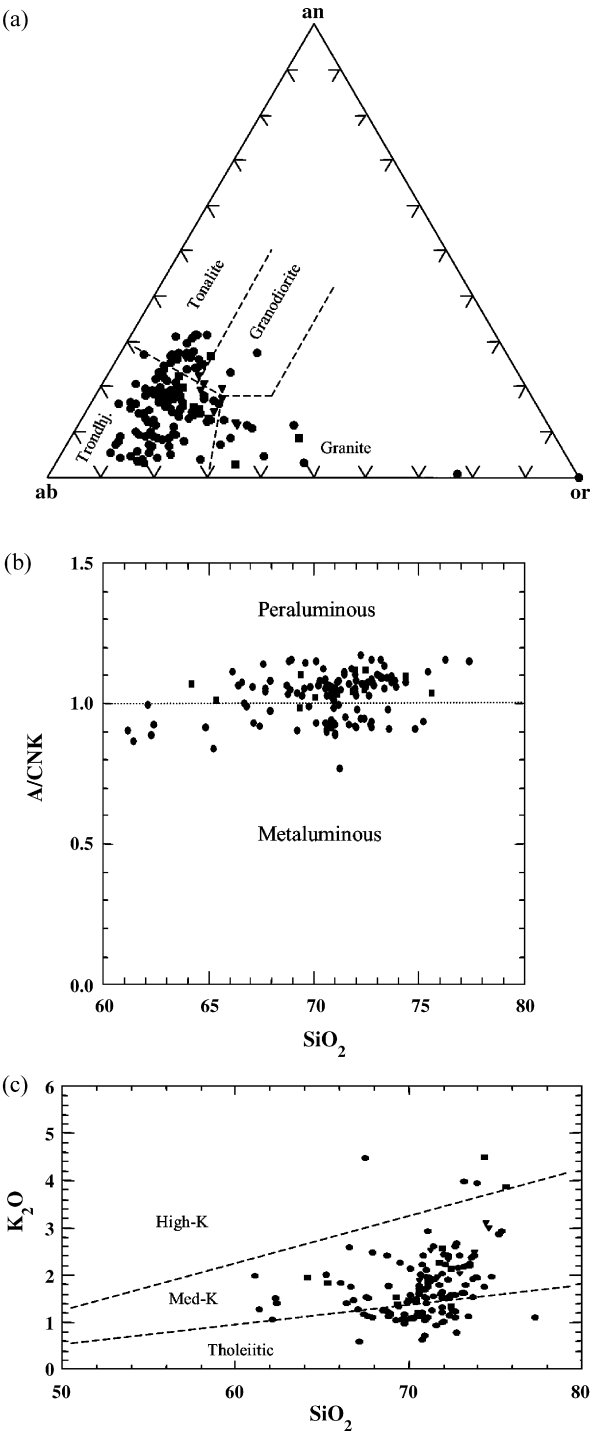

Fig. 2. (a) Classification of the TTG rocks using normative anorthite (an), albite (ab) and orthoclase (or), with fields defined by Barker (1979). Circles, squares: present work; triangles: Anhaeusser and Robb (1983). (b) A/CNK–SiO_2 plot for the TTG rocks. A/CNK = mol $Al_2O_3/(CaO + Na_2O + K_2O)$. (c) K_2O–SiO_2 plot showing the fields defined by Le Maitre et al. (1989). Circles, squares: present work, triangles: Anhaeusser and Robb (1983).

spectrometry system at the University of Stellenbosch. The microscope was operated at 20 kV with a beam current of 120 nA and a probe current of 1.50 nA. Acquisition time was set at 50 s. Spectra were processed by ZAF corrections and quantified using natural mineral standards. This instrument is fitted with a HEXLAND cryostage that allows samples to be cooled to near liquid-N_2 temperature (∼−193 °C), which effectively eliminates Na analytical problems, even when analysing with a fully focussed beam (see, e.g. Vielzeuf and Clemens, 1992).

3.2. Major elements

Major-, trace-element and REE data for the TTG suite are presented in Appendix A in supplementary data. Using the geochemical classification of Barker (1979), the rocks of the TTG suite are classified as mainly trondhjemitic, with minor tonalitic or granitic components of the plutons (Fig. 2a). Their A/CNK values (Fig. 2b) vary between about 0.8 and 1.2. The presence of Hbl, Tit and Mag define these rocks as I-type granites (Chappell and White, 1974), with the implication that they were derived by partial melting of meta-igneous source rocks (Chappell and White, 1984). This suite is low- to medium-K, calc-alkaline (Fig. 2c).

The Harker diagrams in Fig. 3 show the variations of TiO_2, Al_2O_3, Na_2O, CaO, MgO and FeO^T with silica content. SiO_2 contents range from ∼61 to 77 wt%. As is typical for igneous suites, most oxides are negatively correlated with SiO_2. The exceptions are K_2O (Fig. 2c) and Na_2O, with scattered trends. These correlations are generally displayed among the analyses from individual plutons, as well as for the suite, as a whole. Despite the trends displayed for the suite, there is a significant degree of scatter. This point is discussed further below.

3.3. Trace elements

Selected trace-element compositions of the TTG suite are displayed in Fig. 4, plotted as Harker diagrams. Note that, for internal consistency and comparability, all these plots use the XRF analyses and ICPMS REE

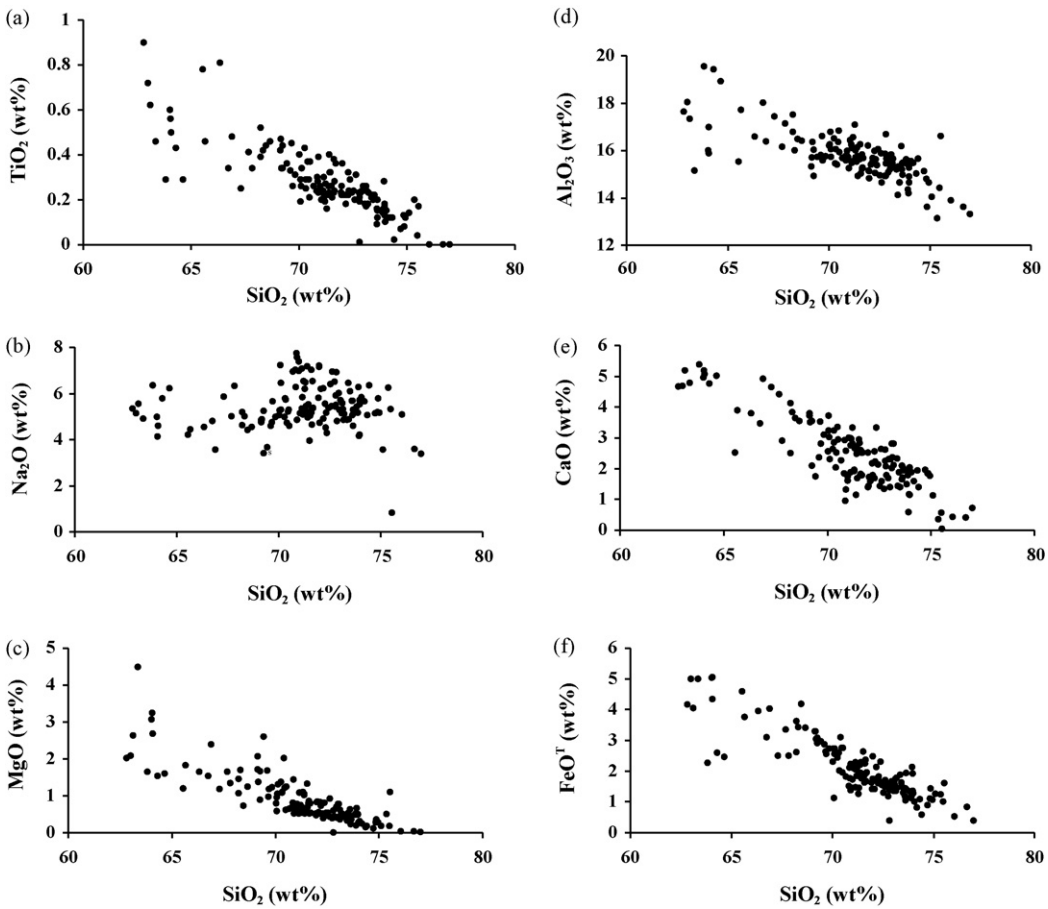

Fig. 3. (a–f) Major-element Harker diagrams for the TTG-suite rocks with $SiO_2 > 60$ wt%, analysed in the present study.

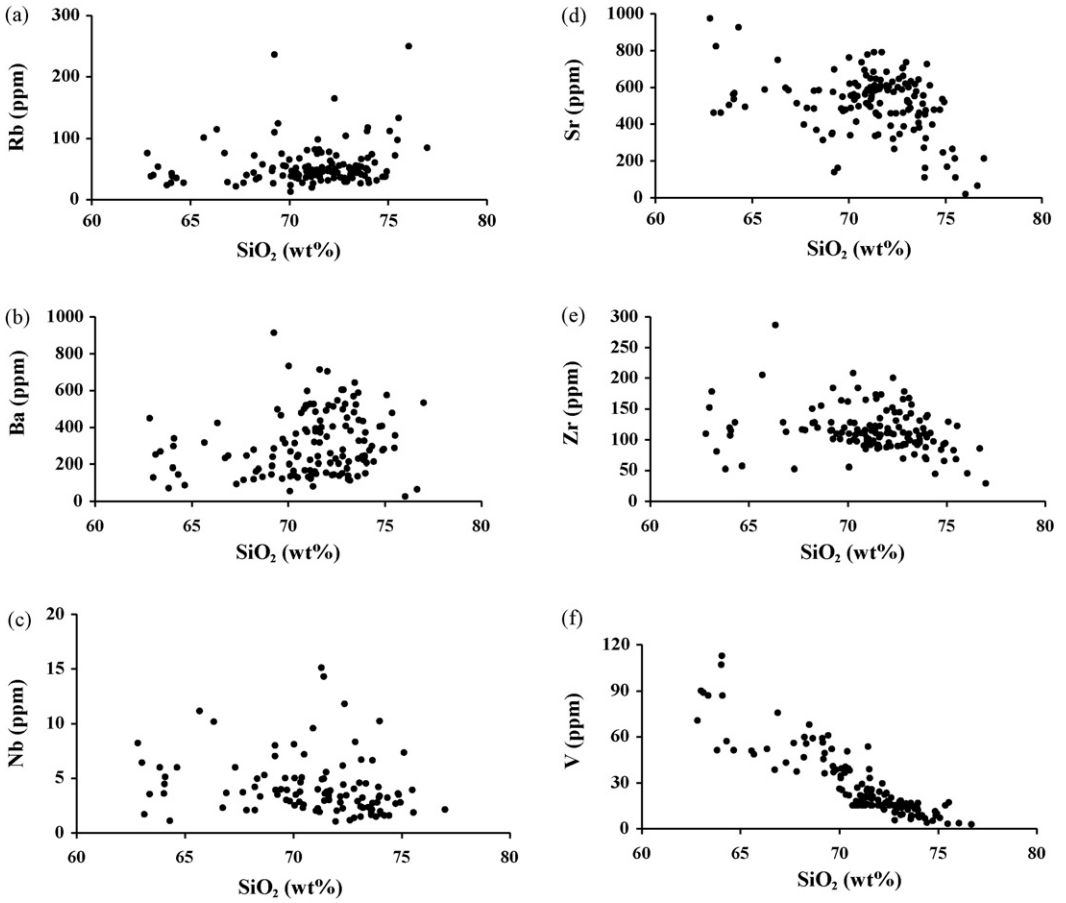

Fig. 4. (a–f) Trace-element Harker diagrams for the TTG-suite rocks with $SiO_2 > 60$ wt%, analysed in the present study.

analyses, presented in Appendix A in supplementary data. For the isotope work (see below) the more accurate isotope-dilution analyses for Sm and Nd are used. The Harker plots typically show scattered distributions. Only V forms a relatively "tight" (i.e. distinct) negative correlation with SiO_2 (Fig. 4f). The data for some individual plutons, however, do exhibit weak trends. However, as a whole, the TTGs do not show tight trace-element trends with SiO_2 content. This suggests that crystal fractionation was not the dominant process in the formation of the TTG suite. The main exception, the trend in V, is probably related to the crystallisation and fractionation of oxide minerals (Fig. 4f). The causes of the geochemical variation are discussed below.

The multi-element diagram of Fig. 5 shows trace element variations normalised to the primitive mantle values of McDonough and Sun (1995). As is common for TTG-like rocks this plot shows considerable enrichment in LILEs and a negative Nb anomaly. Ti, Y and Yb do not show significant enrichments, which is also common in TTG suites. A number of plutons (Steynsdorp, Theespruit, Doornhoek, Batavia and Nelshoogte) also show small depletions (negative anomalies) for Ba, relative to Rb and Th. Compared with the other rocks plotted here, sample BTV13A shows significantly higher enrichments, across the spectrum.

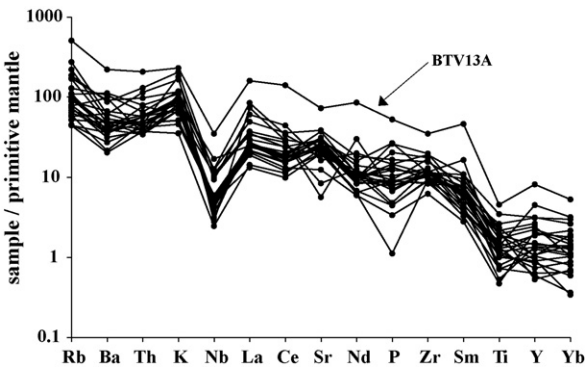

Fig. 5. Multi-element diagram for the TTG rocks, normalised to the primitive mantle values of McDonough and Sun (1995). See text for discussion.

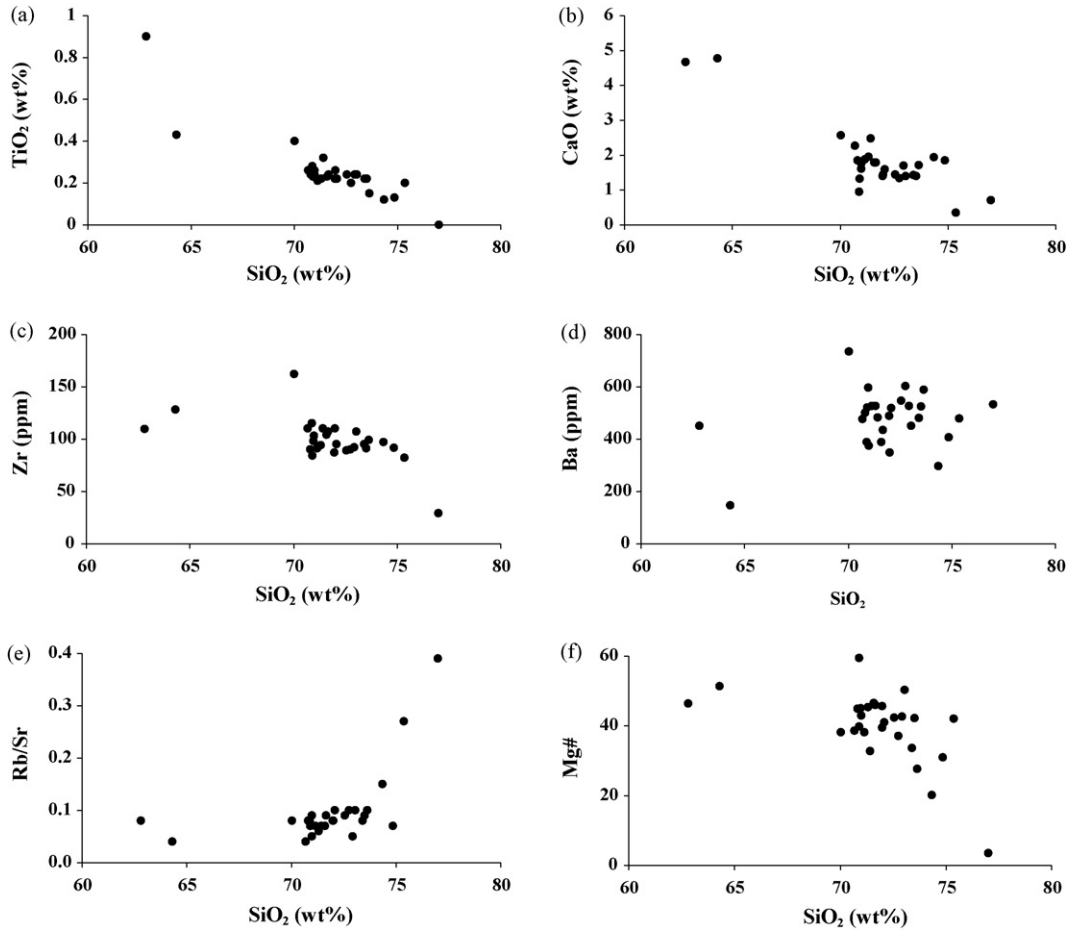

Fig. 6. (a–f) Selected major- and trace-element Harker plots for analyses of rocks from the Stolzburg pluton. See text for discussion.

3.4. Causes of geochemical variation

The plutons of the TTG suite are dominated by the mineral assemblage Pl + Bt ± Hbl, with accessory Ap + Aln + Fe–Ti oxide ± Tit. Crystallisation and fractionation of these minerals could explain the negative trends displayed by CaO, Al_2O_3, MgO, FeO^T, TiO_2 and P_2O_5. Crystal fractionation trends are characterised by quite tight inter-element correlation on Harker plots. Good examples can be found in Wyborn et al. (2001), which deals with differentiation of some mainly felsic plutons in Australia, for which the field, mineralogical and geochemical data are consistent with production of the rock series by crystal fractionation of a single parent magma. For the Barberton TTGs, however, there is generally more scatter in the major-oxide trends than would be expected if crystal fractionation were the sole process responsible for the variation.

As an example of this, Fig. 6 shows selected major- and trace-element Harker plots for analyses of rocks from the Stolzburg pluton. The TiO_2 and CaO and Zr plots seem to suggest quite distinct trends for the rocks of this pluton. Such tight trends (and the MgO trend in Fig. 3b, for example) might be thought of as indicating fractionation. However, if oxides such as Al_2O_3, MgO and FeO^T, are plotted even for genetically unrelated metaluminous felsic rocks, the resulting trends are similar. They probably reflect the stoichiometries of the melting reactions that formed the magmas, and the partitioning of elements between granitic (s.l.) liquids and the residual solids. The melt compositions are quite limited and the residual crystal phases will be similar, especially for variable but generally similar source rock compositions. This effectively buffers the major-element contents of the melts and produces relatively tight major-element trends. This is why the partial melts of a vast range of crustal rock types are broadly granitic in chemistry. The trace elements are not so constrained because their concentrations are commonly not buffered by a crystalline phase that contains the element as a

major structural constituent. Zr is one of the exceptions and, unsurprisingly, Zr trends are usually quite tight on Harker plots. Another factor that contributes to scatter in trace-element concentrations of melts is the apparently common occurrence of disequilibrium during partial melting (e.g. Bea, 1996). In the CaO plot for Stolzburg (Fig. 6b), note that rocks with around 70–71 wt% SiO_2, have CaO contents varying from about <1 to >2.5 wt%. This is a little more scatter than might be expected in a series of rocks related by fractional crystallisation, magma mixing or crystal unmixing. If plagioclase is not present in the residual assemblage of the TTG source rocks (as seems certain, for most), CaO will be only weakly buffered, perhaps by clinopyroxene in the melting residue, and scatter is expected. The Ba plot (Fig. 6d) shows a large amount of scatter, with no clear trend. This degree of scatter and lack of a trend is also unusual for Ba in differentiated magmatic suites. Note that the Rb/Sr shows a flat trend that only kicks upward at the very high-SiO_2 end (Fig. 6e). Even then, not all of the rocks with SiO_2 >74 wt% form part of this upward spike. Note also that the variation in Mg# (Fig. 6f) shows only a rough negative correlation with SiO_2 and has a great degree of scatter (e.g. Mg# varying between 27.67 and 50.23 at SiO_2 contents close to 73 wt%). Again this is abnormal for variation controlled by mixing or crystal fractionation processes.

We interpret these variations as most probably due to initial variation among the magma fractions that formed the TTG plutons, i.e. that the Stolzburg pluton was probably assembled by the aggregation of a number of different magma batches, each with a slightly different melt composition. Evidence is accumulating that this is the case for very many felsic intrusive bodies (e.g. Glazner et al., 2004; Clemens et al., in press). The observed overall trends of increasing CaO, FeO and MgO contents,

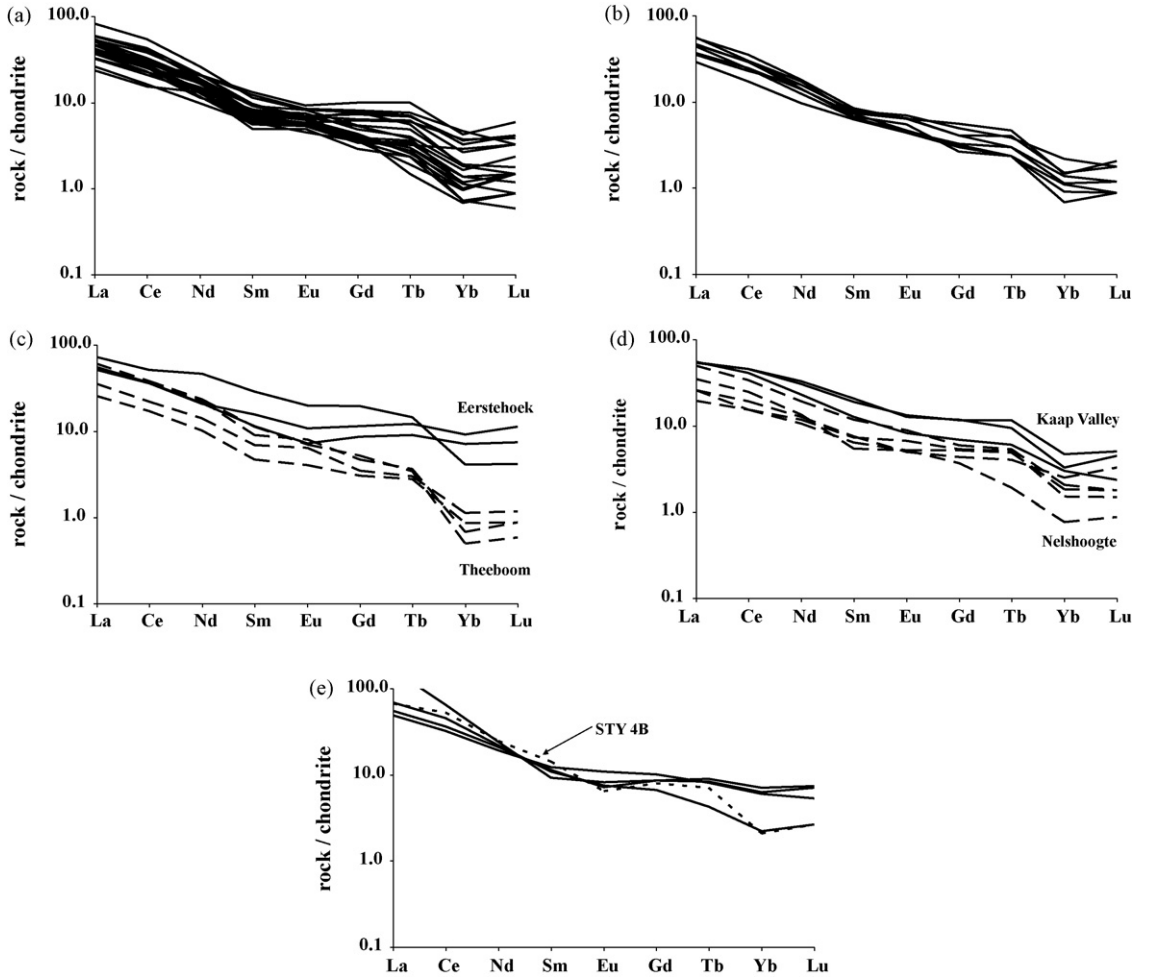

Fig. 7. REE patterns for the TTG plutons normalised to chondrite (Nakamura, 1974; Haskin et al., 1968, for Tb); (a) Batavia, Badplaas and Rooihoogte, (b) Stolzburg and Theespruit, (c) Eerstehoek and Theeboom, (d) Kaap Valley and Nelshoogte, (e) Steynsdorp and Doornhoek.

with decreasing SiO_2 and Na_2O are most probably due to progressive partial melting, with incremental melt extraction. However, the scattered geochemical variation in the TTG rocks represents an overtone that is probably due to local variations in the compositions of the sources of individual magma batches. These separate batches evidently failed to mix efficiently within the growing plutons. Intraplutonic intrusive relationships between different magma batches clearly demonstrate that several of the TTG plutons are composite bodies. Such geochemical and geological relationships are present in the Badplaas, Theespruit and Nelshoogte plutons.

3.5. Rare earth elements

Fig. 7 shows the REE patterns for samples from the TTG plutons. The samples are LREE-enriched and HREE-depleted (relative to chondritic concentrations), producing average $(La/Yb)_N$ values of 17–49 and Yb_N values of 1–10. However, Eerstehoek (Fig. 7c), Steynsdorp and Doornhoek (Fig. 7e) and some samples from Kaap Valley exhibit flatter trends than the rest of the plutons.

Depletion in the HREE, with respect to chondritic concentrations, is usually interpreted as a source-related feature due to preferential partitioning of these elements into coexisting restitic garnet. Rapp et al. (1991) produced TTG-like liquids with $Yb_N < 3$ in his high-*T*, fluid-absent partial melting experiments on metabasalts, at pressures within the garnet stability field. Although Yb_N varies from about 1–10 in individual Barberton TTG samples, the plutons have average Yb_N values varying from 1.19 (Theeboom) to 3.84 (Kaap Valley), with an overall average of 2.61. The average Archaean amphibolite (Gao et al., 1998) has $Yb_N \approx 12$, which suggests that the Barberton TTG magmas were mostly depleted in HREE with respect to their possible source rocks, though by varying amounts for different plutons. This is consistent with garnet-bearing residues, with some variation in the proportion of garnet.

Published REE partition coefficients for hornblende and plagioclase (summarised in Rollinson, 1993) suggest that the presence of a large amount of hornblende as a residual mineral in the magma source could negate the influence of a small amount of residual plagioclase, producing a melt lacking a negative Eu anomaly. However, Rapp and Watson (1995) showed that fluid-absent partial melting of metabasic rocks only produces TTG-like liquids (and melts of any significant quantity) at temperatures above amphibole stability. Thus, we infer that large amounts of residual hornblende are unlikely to have been present. Thus, the observed lack of Eu anomalies is best interpreted as indicating the absence of plagioclase in the residual source. In addition, fractionation of a sufficient quantity of hornblende, from a felsic magma, to overcome the effect of plagioclase fractionation, is not feasible, on simple mass-balance grounds. The magmas could not have contained sufficient ferromagnesian component and, in any case, the hornblende in the Barberton TTG rocks is not an early-crystallising phase. Thus, the rarity of negative Eu anomalies suggests that it is unlikely that plagioclase fractionation occurred during the evolution of most Barberton TTG magmas. The somewhat flatter REE patterns for Eerstehoek, Steynsdorp, Doornhoek and Kaap Valley may signify a lower abundance of garnet in the restitic source of these magmas. Anhaeusser and Robb (1983) analysed a number of TTG samples from the same area but, for internal consistency, their data are not plotted in Fig. 7. Nevertheless, these authors record negative Eu anomalies (average Eu/Eu^* values of 0.72–0.83) in a few samples from the Steynsdorp and Doornhoek plutons, suggesting a degree of plagioclase fractionation. This is compatible with petrographic and textural evidence for the early crystallisation of plagioclase in the rocks.

Four of the analysed samples in our dataset (Appendix A in supplementary data) have high K_2O/Na_2O (>1), and thus could be considered not to belong to the TTG suite. Batavia pluton sample BTV13A has a relatively low SiO_2 content (65.55 wt%) and $K_2O/Na_2O = 1.21$. It is characterised by extremely elevated P_2O_5, Ba, Rb, Sr, Y, Zr, Nb, Zn and ΣREE but lacks a positive Eu anomaly. These features, well portrayed in Fig. 5, are consistent with a rock enriched in biotite, zircon, apatite and Fe-Ti oxides. We interpret this as a cumulate, derived from the TTG magma by magmatic segregation of these phases; it is not plotted in Fig. 7. The remaining three samples in this category (NLG9, STY4B and STZ23) all have very high SiO_2 contents (>75 wt%). The REE pattern for STY4B is shown as the dashed line in Fig. 7e). This rock has a high SiO_2 content (75.11 wt%), elevated K_2O/Na_2O (1.28), relatively high Ba and low concentrations of Sr, Y and V. Its REE pattern is unexceptional, but there is a shallow negative Eu anomaly. All of this is consistent with an origin as a felsic differentiate of a TTG magma; STZ23 is similar. However, sample NLG9 has extreme K_2O/Na_2O (4.86), high Rb, low Sr, high ΣREE and rather elevated LREE contents. It is also strongly peraluminous (A/CNK = 2.88). These characteristics suggest that the NLG9 magma was probably formed by partial melting of a minor metasedimentary component within the TTG source region.

In summary, the generation of the majority of the TTG magmas probably involved partial melting of mafic

Table 1
Nd isotope data for Barberton TTG plutons

Sample	Pluton	Nd (ppm)	Sm (ppm)	$^{147}Sm/^{144}Nd_{rock(0)}$	$^{143}Nd/^{144}Nd_{rock(0)}$	±2 se	$^{143}Nd/^{144}Nd_{rock(t)}$	t (Ga)[a]	$\varepsilon Nd(t)$[b]
NLG1	Nelshoogte	9.933	1.518	0.09236	0.510323	20	0.508348	3.236	−1.64
NLG13	Nelshoogte	12.089	2.120	0.10596	0.510618	15	0.508352	3.236	−1.56
NLG25a	Nelshoogte	7.683	1.884	0.14817	0.511474	41	0.508305	3.236	−2.48
STZ1	Stolzburg	7.240	1.210	0.10070	0.510448	35	0.508153	3.445	−0.07
STZ18	Stolzburg	8.890	1.520	0.10330	0.510566	23	0.508211	3.445	1.09
TBM1b	Theeboom	7.208	1.387	0.11631	0.510740	27	0.508090	3.445	−1.30
TP21[c]	Theespruit	7.810	1.550	0.12020	0.511076	24	0.508339	3.443	3.54
TP30[c]	Theespruit	8.980	1.610	0.10840	0.510814	10	0.508345	3.443	3.67

[a] U-Pb zircon ages from Armstrong et al. (1990), Kamo and Davis (1994), Kröner et al. (1991, 1996).
[b] Calculated using present day chondritic values of $^{143}Nd/^{144}Nd = 0.512638$ and $^{147}Sm/^{144}Nd = 0.1967$; $^{147}Sm/^{144}Nd_{rock(0)}$ = the Sm/Nd isotopic ratio of the rock sample at present time; $^{143}Nd/^{144}Nd_{rock(0)}$ = the Nd isotopic ratio of the rock sample at present time (i.e. $t = 0$); $^{143}Nd/^{144}Nd_{rock(t)}$ = the Nd isotopic ratio of the rock sample at time t; $\varepsilon Nd(t) = [^{143}Nd/^{144}Nd_{rock(t)}/^{143}Nd/^{144}Nd_{CHUR(t)} - 1] \times 10^4$.
[c] Samples collected by C. Anhaeusser.

source rocks with production of a garnet-bearing restite. In general, plagioclase was not a major phase in the residual source nor was it a fractionating phase during magma evolution. The exceptions are the Steynsdorp and Doornhoek plutons, in which there is some geochemical evidence for minor plagioclase fractionation or perhaps a small amount of plagioclase in the residuum. The relatively flatter REE patterns of rocks from these two plutons imply that the restite produced during their generation was relatively garnet-poor. There is geochemical evidence for the presence of a minor metasedimentary component in the TTG magma source region, specifically for the rocks of the Nelshooghte pluton. The compositions of the residua are important because their mineralogy provides constraints on the depths (pressures) at which the TTG magmas were generated. Garnet is stable at relatively high pressures in metabasic rocks, such as the sources of TTG magmas. For fluid-absent partial melting of metabasites, at 1000–1150 °C, Rapp et al. (1991) and Rapp and Watson (1995) showed that pressures >0.8 GPa (about 30 km) are required to stabilise garnet, and ≥1.2 GPa (about 40 km) for garnet to be stable in the absence of plagioclase. Plagioclase disappears from the phase assemblage by dissolution in the melt, at high T, and by breakdown to jadeitic pyroxene and the grossular component in garnet, towards high P. The Rapp and Watson (1995) experiments on an Archaean greenstone (Fig. 2, op. cit.) show a window for simultaneous garnet presence and plagioclase absence at $T > 1000$ °C and P between 1.2 and 2 GPa. As noted above, the chemistry of most of the Barberton TTG rocks strongly suggests that the melts equilibrated with plagioclase-free, garnet-bearing residual source assemblages. From this we suggest that most of the Barberton TTG rocks were derived from sources located at depths of at least 40 km. The metamorphic and structural studies cited above suggest that this melting occurred in thickened crust. The Steynsdorp and Doornhoek magmas may have been derived from slightly shallower depths, where residual garnet was present in smaller quantities, perhaps accompanied by a small amount of plagioclase.

3.6. Nd isotopes

Systematics of the Sm–Nd isotope system are used to calculate εNd at the known crystallisation ages of the plutons concerned (Kamo and Davis, 1994). The calculated $\varepsilon Nd(t)$ values are presented in Table 1 and Fig. 7, and range from +3.67 to −2.48. For comparison, the $\varepsilon Nd(t)$ values for the greenstone volcanic samples from the Onverwacht Group (Hamilton et al., 1979) are also included. These were calculated using recent U-Pb zircon dates (Armstrong et al., 1990). Also marked on the diagram are lines representing CHUR ($\varepsilon Nd = 0$) and the evolution of the depleted mantle, as defined by Goldstein et al. (1984), which assumes a linear increase in εNd, from a chondritic value at 4.5 Ga to a present day value of +10.

From Fig. 8 it is clear that most of the analysed ~3.45 Ga TTGs have positive εNd values. This suggests that they were derived either from the mantle directly, or from a juvenile crust that had not long been separated from the mantle. This is consistent with the published view that the Theespruit Formation represents an accreted oceanic arc fragment (De Wit et al., 1987). The Stolzburg pluton, in particular, exhibits a close similarity to the basalts and komatiites of the Theespruit (Tspt), Komati (Kom) and Hoogenoeg (Hoog) Formations (Hamilton et al., 1979). Its values typically lie between those of CHUR and the depleted mantle. On this evidence, it seems possible that greenstone rock types may be the sources of the TTG magmas.

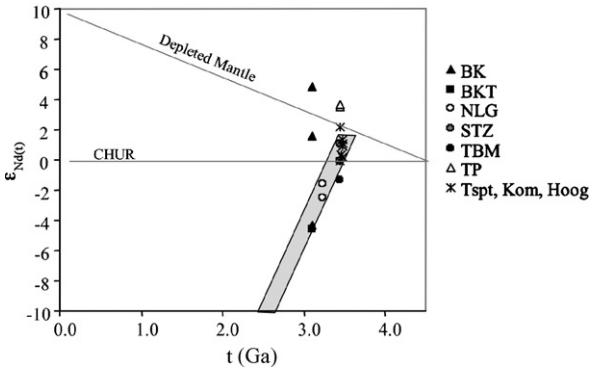

Fig. 8. Graph showing εNd vs. age (Ga) of the Barberton granitoid rocks. BK and BKT: members of the potassic granitic suite, NLG: Nelshoogte, STZ: Stolzburg, TBM: Theeboom, TP: Theespruit, Tspt: Theespruit Formation, Kom: Komati Formation, Hoog: Hoogenoeg Formation.

3.7. Implications of the geochemical results

The lack of major- and trace-element evidence for mineral fractionation in the petrogenesis of most of the Barberton TTG plutons suggests that the most of the measured rock compositions probably reflect magma compositions. This is consistent with the interpretation that the differences in chemistry between plutons of the same age also reflect separate, contrasting magma batches, and that the scattered trends within the plutons probably reflect heterogeneities within their source rocks, retained through incomplete magma homogenisation. The εNd values suggest that the TTGs were derived from juvenile crustal sources with depleted-mantle signatures. The similarity between the εNd values of the ∼3445 Ma TTGs and the Lower Onverwacht greenstones further implies that the greenstone materials could be the sources of these magmas, if they were present at the required depths. REE data suggest that the TTG magmas were mostly generated at depths where garnet was stable and formed part of the melting residue.

Trace- and rare earth-element modelling is helpful in constraining the actual composition of the restite. Fig. 9 compares the chondrite-normalised La/Yb ratios ($(La/Yb)_N$) and Sr/Y ratios of the Barberton granitoids. It highlights the fact that the TTG suite has low Yb_N and Y values and highly evolved $(La/Yb)_N$ and Sr/Y ratios, typical of Archaean TTGs (Martin, 1986). The arrows on the diagrams represent batch melting trends for Archaean tholeiites that produce restite compositions of amphibolite, and 7–30% garnet-rich amphibolite or eclogite, as modelled by Petford and Atherton (1996), Atherton and Petford (1993), Martin (1986) and Drummond and Defant (1990). Due to a lack of data for Barberton amphibolites, we cannot calculate a model that is more specific to this area. However, the differences are unlikely to invalidate the general observations. Using the literature-derived trends as a guide, it appears that the TTG suite could have been derived through partial melting of a primitive basaltic source, producing an amphibolitic or eclogitic restite with >30% garnet (Fig. 9).

The likelihood that the Barberton TTGs represent relatively little-modified initial magma compositions, coupled with the inference of an initial magma in equilibrium with garnet, raises the possibility of establishing the minimum pressure of magma genesis, using experiments to establish the lowest pressure at which garnet would be stable in the TTGs. This is perhaps a more accurate way of determining pressure of genesis than establishing the pressure of garnet appearance in a general metamafic protolith. This is because the specific protolith composition is unknown, and garnet stability is sensitive to a

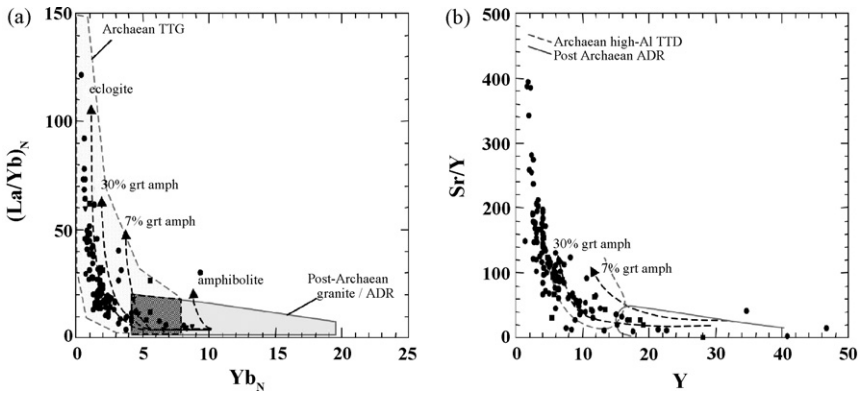

Fig. 9. (a) $(La/Yb)_N$–Yb_N and (b) Sr/Y–Y diagrams for the TTG rocks. Arrows indicate the batch melting pathways of Archaean tholeiites with source mineralogies of amphibolite, 7–30% garnet-rich amphibolite or eclogite (adapted from Petford and Atherton, 1996). Archaean TTG/high-Al trondhjemite-tonalite-dacite (TTD) and post Archaean granite/andesite-dacite-rhyolite (ADR) fields adapted from, e.g. Martin (1986), Drummond and Defant (1990), Atherton and Petford (1993), Petford and Atherton (1996). Dark shading: overlap area between the TTG and ADR fields.

number of subtle geochemical variations in metabasic rocks.

4. Experiments

4.1. Starting materials

4.1.1. Garnet stability in TTG rocks

A specimen from the Theespruit Pluton (THE4A) was chosen as the starting material for this series of experiments. We selected a rock that we judged most likely to be representative of a TTG magma that had undergone little modification by fractional crystallisation. Thus, the sample has relatively low SiO_2 (~70 wt%), high Mg# (49), normal K_2O (~1.6 wt%) and P_2O_5 (0.08 wt%), and minimal evidence for secondary alteration. THE4A contains plagioclase (An_{15}), quartz, biotite (Mg# = 52), minor hornblende (Mg# = 54), minor microcline (Or_{96}) and accessory apatite, allanite and epidote (Fig. 10). Although the rock shows signs of alteration, with minor sericitisation of plagioclase, it represents the freshest sample collected from the Theespruit pluton. Bulk rock and mineral geochemical compositions are shown in Tables 2 and 3, respectively.

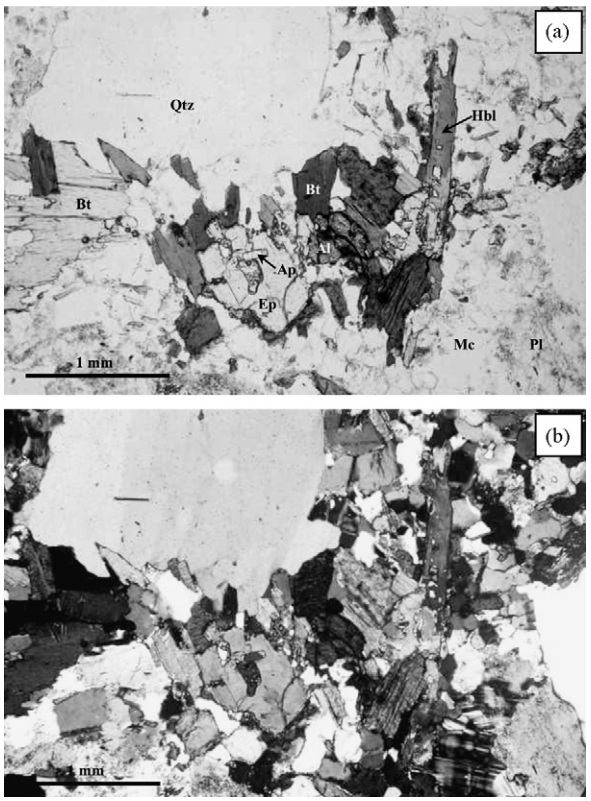

Fig. 10. Photographs illustrating the mineralogy of experimental starting material THE4A, (a) in plane polarised light and (b) under crossed polars. Pl: plagioclase, Mc: microcline, Qtz: quartz, Bt: biotite, Hbl: hornblende, Ap: apatite, Ep: epidote, Al: allanite.

Table 2
Major element and CIPW normative compositions (100% anhydrous) of the starting materials for the experiments and the average Theespruit Formation greenstone

	THE4A	AmX12-a	Ave greenstone[a]
SiO_2	70.33	53.81	54.31
TiO_2	0.24	0.79	1.14
Al_2O_3	16.04	13.71	12.85
FeO^T	2.00	9.13	12.13
MnO	0.03	0.28	0.29
MgO	1.11	10.09	7.97
CaO	2.85	9.41	8.92
Na_2O	5.74	2.05	1.68
K_2O	1.56	0.55	0.54
P_2O_5	0.08	0.17	0.17
q	22.01	1.89	6.14
or	9.24	3.25	3.19
ab	48.54	17.97	14.76
an	13.34	25.96	25.38
di	0.27	15.48	14.27
hy	5.94	33.56	33.70
il	0.47	1.50	2.17
ap	0.18	0.39	0.39
Mg#	49	66	54[b]
K_2O/Na_2O	0.27	0.27	0.32
A/CNK	0.98	0.65	0.66

FeO^T = total Fe as FeO.
[a] Average of nine analyses.
[b] Range = 20–71.

4.1.2. Partial melting of amphibolite

Partial melting of amphibolitic rocks has been well studied since the 1970s, with an emphasis on fluid-absent phase relations since the 1990s. Recently, Clemens (2005) and Moyen and Stevens (2005) summarised the data on phase relations, melt proportions and their evolution with *T*, and melt compositions. For fluid-absent conditions, Moyen and Stevens (2005) found that, at *T* near 900 °C, the pressure of the garnet-in phase boundary varies between <1.0 and 1.4 GPa, as a function of the composition of the starting rock. Likewise, the positions of the solidus and the amphibole-out boundaries also vary substantially. Thus, despite the volume of this previous work, it seems useful to experimentally investigate the partial melting behaviour of the Barberton amphibolite. This is because these rocks are relatively low in Al_2O_3, and have high Mg#s, features uncommon among previously studied compositions.

The Theespruit Formation is the portion of the Barberton greenstone belt that experienced the highest grade of metamorphism, and is the only part of the

Table 3
Compositions of minerals in the starting materials

	THE4A				AmX12-a	
	Hbl	Bt	Pl	Kfs	Hbl	Pl
n	1	4	2	2	6	2
SiO_2	46.13	36.93	64.95	64.11	46.74	67.94
TiO_2	0.24	1.66	0.10	0.02	0.97	0.19
Al_2O_3	9.51	15.58	21.76	18.29	10.56	21.24
Cr_2O_3	0.08	0.10	–	–	0.14	–
Fe_2O_3	4.26	0.00	–	0.15	3.30	–
FeO	15.27	19.64	0.08	–	10.44	0.21
MnO	0.45	0.33	–	–	0.29	–
MgO	10.18	11.92	0.11	0.00	13.06	0.03
CaO	12.40	0.20	3.20	0.05	12.46	1.27
Na_2O	1.19	0.21	9.68	0.45	1.27	10.76
K_2O	0.88	9.43	0.11	16.42	0.63	0.32
Total	100.59	96.00	100.01	100.21	99.86	101.94
xO^{2-}	23	22	8	8	23	8
Si	6.730	5.417	2.862	2.983	6.679	2.924
Ti	0.026	0.183	0.003	0.001	0.104	0.006
Al	1.635	2.695	1.130	1.003	1.779	1.077
Cr	0.009	0.011	–	–	0.015	–
Fe^{3+}	0.467	–	–	0.005	0.356	–
Fe^{2+}	1.863	2.411	0.003	–	1.249	0.008
Mn	0.056	0.042	–	–	0.035	–
Mg	2.214	2.608	0.007	–	2.782	0.002
Ca	1.938	0.032	0.151	0.002	1.908	0.058
Na	0.337	0.061	0.827	0.040	0.352	0.898
K	0.164	1.762	0.007	0.975	0.114	0.017
ΣCations	15.44	15.24	4.99	5.02	15.37	4.99
Mg#	54	52	–	–	68	–
Fsp comp.			An_{15}	Or_{96}	–	An_6

Onverwacht Group whose mineral assemblages record upper amphibolite-facies metamorphic conditions. This results from the fact that it formed part of the 'lower plate' during 3.23 Ga tectonism, was decoupled from the rest of the greenstone belt and experienced a separate, higher-grade history, along with the high-grade southern granitoid gneiss terrain (Dziggel et al., 2002; Kisters et al., 2003; Diener et al., 2005). Felsic volcanic rocks within the Theespruit Formation show strong geochemical similarities with the TTG rocks of the Steynsdorp pluton (e.g. HREE depletion and absence of any marked Eu anomaly; Diener, 2004), and so may be older that the Stolzburg and Theespruit plutons. These relationships indicate that mafic rocks from the Theespruit Formation could be the sources for both the 3.45 and 3.23 Ga TTG magmas.

An amphibolite sample (AmX12-a) was therefore taken from one of the large greenstone remnants enclosed within the Batavia pluton (Fig. 1). For purposes of comparison, its bulk composition is given in Table 2, along with the average of nine other mafic rocks from the Theespruit Formation. Its Mg# lies close to the middle of the wide range for these rocks (footnote in Table 2) and, apart from marginally higher Na_2O and lower TiO_2, AmX12-a is typical of Theespruit mafic rocks, and indeed of some other Barberton greenstones. Partial melting experiments on this material, at appropriate *P*, *T* and fluid conditions should therefore provide us with an answer to the question of whether these rocks could have been the source for the Barberton TTGs. They also make a useful contribution to the overall dataset on amphibolite melting relations.

Most amphibolite-facies Barberton greenstones carry some greenschist-facies retrograde overprint. In AmX12-a this was marked by minor replacement of hornblende by chlorite and plagioclase by epidote. Since the presence of these lower-grade minerals increases the H_2O content of the sample, over that which would apply to progressively metamorphosed equivalents in the upper amphibolite facies, the sample needed to be

amphibolitised prior to using it as a starting material. This was achieved by placing it in a gold capsule, and annealing it in an internally heated gas vessel, at 650 °C and 0.2 GPa, for 7 days. The resulting mineralogy was ~70% amphibole (Mg# = 68) and ~30% plagioclase (An_6), with traces of K-feldspar. Bulk-rock and mineral chemical compositions are given in Tables 2 and 3, respectively.

4.2. Pressure, temperature and fluid conditions

4.2.1. Garnet stability in TTG

In metaluminous rocks, the stability of Mn-poor garnet depends primarily on pressure. Therefore, we kept the temperature constant in this first series of experiments. A temperature of 875 °C was chosen because this would be near the TTG liquidus at the chosen H_2O content of the system (see below). Pressure was initially set at 1 GPa and then varied, by increments of 0.1 GPa, between 1.2 and 1.7 GPa, until the initial appearance of garnet was tightly constrained.

A key assumption of this work is that a source rock of amphibolitic composition partially melted, under fluid-absent conditions, to form TTG magma. In the Archaean, with the possibility of higher geothermal gradients than at present, this sort of high-*T* melting could conceivably occur in a subducting slab (e.g. Martin, 1994), in the roots of oceanic plateaux (e.g. Condie, 2005) or in the deep crust of the thickened upper plate (e.g. Petford and Atherton, 1996). Stevens and Clemens (1993) and Clemens and Watkins (2001) reviewed the evidence for the dominance of fluid-absent conditions during the formation of granitoid magmas by crustal melting. Under these conditions, the hydrous minerals provide the H_2O component required to form hydrous granitoid melts. The magma from which THE4A crystallised would have contained far more H_2O than is now present in the hydrous minerals of the rock. The average initial H_2O content of granitoid magmas is ~4 wt% (Clemens, 1984). Thus, H_2O must be added to the system to replicate the true initial TTG magma composition.

An estimate of the amount of H_2O in the assumed amphibolitic source rock leads to an approximation of the amount of H_2O present in the melt. Calculations were made on the basis of 25% partial melting of amphibolite, at 900 °C and 1 GPa, with complete destruction of the hornblende. Using the model of Clemens and Vielzeuf (1987), this would require 1.4 wt% of H_2O in the source rock. For fluid-absent melting, melt proportion (wt%) = H_2O content of rock/H_2O content of melt formed (Clemens and Vielzeuf, 1987). Thus, the amount of H_2O required in the TTG melt would be 5.6 wt% (at 900 °C and 1 GPa). The H_2O content of the bulk rock derived from biotite (~15 vol%) already present in the starting material, would be about 0.6 wt%. Thus, we would need to add 5 wt% H_2O to an experimental charge, in order to obtain approximately the correct overall H_2O content. We chose to use an experimental charge of 0.01 g of TTG rock powder so this would require the addition of ~0.5 μL (i.e. 5 wt%) of high-purity deionised H_2O. The first experiment, using 0.5 μL of added H_2O, and run at 875 °C and 1 GPa, produced only glass, indicating super-liquidus conditions. The H_2O content was subsequently reduced to 0.4 μL (i.e. 4 wt%), which ensured that there would be at least some crystals present. Note that no free fluid phase was present in any of the near-liquidus TTG experiments; all H_2O was dissolved in the melt phase.

The philosophy behind these phase equilibrium experiments is that, at the pressure and temperature at which a magma is generated, the melt will be in equilibrium with the mineral phases that constitute the restite. If the magma then remained near its site of generation and crystallised, the near-liquidus phases would mimic the phases in the restite. Thus, if we can determine the minimum pressure at which garnet appears near the liquidus of a Barberton TTG, we will obtain an estimate of the minimum pressure at which the TTG magma was generated.

4.2.2. Partial melting of amphibolite

We also took the Barberton basaltic greenstone amphibolite (AmX12-a) and subjected it to the metamorphic conditions suggested by the results of the TTG near-liquidus experiments. The compositions of partial melts of this basaltic amphibolite can be compared with the compositions of the TTG rocks, to determine whether Barberton amphibolites, such as this, could have been the sources of some of the Barberton TTG magmas. The pressure used for the partial melting experiments was based on the results of the near-liquidus experiments. Conditions were set at 1.6 GPa, and melting temperatures of 875, 925 and 1000 °C were investigated. This temperature range is appropriate to the production of partial melts from amphibolitic source materials (see, e.g. Clemens, 2005; Moyen and Stevens, 2005), and allowed us to assess the effect of *T* on the degree of melting, the compositions of melts, and stability ranges of minerals in the melting interval. In fluid-absent partial melting, the hydrous character of any partial melt is derived through breakdown of crystalline hydrates, in this case hornblende. Thus, no additional H_2O was added to the experimental charges in this series of experiments.

4.3. Experimental methods

The powdered starting materials were finely ground, in a mechanical agate mortar, to an average grain size of ~5 μm, dried at 110 °C and stored, over silica gel, in a vacuum desiccator. Gold capsules (10 mm long, 3 mm OD and 0.15 mm wall thickness) were used to contain the samples plus any added H_2O. Au is unreactive, does not strongly absorb Fe from the sample, inhibits H_2 diffusion and thus preserves fO_2 at realistic reducing levels. Based on previous studies of the redox conditions in this piston-cylinder apparatus, $\log fO_2$ is believed to lie between QFM and QFM-2 (Graphchikov et al., 1999). Each capsule was annealed and arc welded at one end prior to the addition of ~0.01 g of powdered sample. For experiments with added H_2O, deionised water was loaded into the capsule, before the powder, using a 10 μL syringe. These capsules were sealed by arc welding with the lower end submerged in a water bath, to cool the capsule and prevent boiling and loss of fluid. For the fluid-absent melting experiments on the greenstone amphibolite, the powder was added, the open end of the capsule gently crimped shut and the capsule dried, at 110° for 30 min, prior to final arc welding.

Experiments were carried out in a 12.7 mm diameter, non-end-loaded, piston-cylinder apparatus (Depths of the Earth Company, Tempe, Arizona, USA). NaCl-Pyrex cells were used for experiments above 900 °C. For lower-temperature runs NaCl-only cells were used. Thermocouples were type-K (chromel-alumel), and temperatures are considered to be accurate to ±1 °C. Precision in pressure control varied between different experiments but was generally around ±0.05 GPa. The Au capsules were flattened and folded into small packets, the sides of which rested flat in the cells, separated from the thermocouple tip by a thin disk of alumina. Experiments were run for 96 h and quenched isobarically, until T fell to about 600 °C, to prevent vesiculation of any glass present, as a result of volatile exsolution. When the runs were completed, the capsules were removed from the cells, cleaned, opened and the contents examined. A part of each run product was hand-ground in an agate mortar and a grain mount made, for examination with an optical microscope. Another intact piece of the run product was mounted in epoxy resin, sectioned and polished for analysis with the SEM/microprobe.

5. Results

5.1. TTG near-liquidus experiments

All experimental conditions and run products are given in Table 4. Note that because the starting material was crystalline (effectively seeded with plagioclase), we can be reasonably confident that the absence of plagioclase in the run products reflects its instability under these P–T–aH_2O conditions. The pressure for the appearance of near-liquidus garnet is constrained to 1.52 ± 0.05 GPa, which equates to a depth of 51 ± 2 km (assuming a largely mafic crust with a density of 3000 kg/m^3). Due to the importance of the minimum pressure for the appearance of near-liquidus garnet, we compared the experimental result with the prediction of the Perple_X linear programming package (see, e.g. Connolly, 2005) for calculation of phase diagrams using thermodynamic properties of minerals and melts. We used the bulk composition of THE4A, with total H_2O in the system set at 4.42 wt%, as in the experiments. Phases considered in the calculations were Qtz, Pl, Kfs, Bt, Hbl, Grt, Cpx, Opx and melt. The silicate melt composition was fixed as the composition found experimentally, in run PC1-073 (Table 5). The predicted pressure for the

Table 4
Experimental conditions and run products

Run no.	Sample composition	P (MPa)	T (°C)	Duration (h)	Run products
PC1-069	THE4A[a] + 0.5 μL H_2O[b]	989 ± 23	875 ± 1	96	melt
PC1-070	THE4A[a] + 0.4 μL H_2O[b]	1184 ± 12	875 ± 1	96	Cpx, Hbl, melt
PC1-075	THE4A[a] + 0.4 μL H_2O[b]	1407 ± 22	875 ± 1	96	Hbl, melt
PC1-077	THE4A[a] + 0.4 μL H_2O[b]	1474 ± 22	875 ± 1	96	Cpx, Hbl, melt
PC1-080	THE4A[a] + 0.4 μL H_2O[b]	1574 ± 22	875 ± 1	96	(Grt), Hbl, melt
PC1-073	THE4A[a] + 0.4 μL H_2O[b]	1717 ± 29	875 ± 1	112	Grt, Cpx, Hbl, Ru, melt
PC1-083	AmX12-a	1598 ± 24	875 ± 1	96	Grt, (Ru), (Ap), Opx, Cpx, Hbl, Qtz, melt
PC1-086	AmX12-a	1596 ± 20	925 ± 1	96	Grt, (Ru), (Ap), Opx, Cpx, Hbl, melt
PC1-087	AmX12-a	1581 ± 47	1000 ± 1	96	Grt, (Ru), (Ap), Opx, Cpx, melt

NB parentheses indicate minor amounts of the phase present.
[a] 0.01 g powdered rock.
[b] H_2O added to capsules but all runs fluid-absent at P and T (with ~4 wt% or ~5 wt% H_2O in the melt, near the liquidus).

Table 5
Average major-element[a] and CIPW normative compositions of the melts produced in near-liquidus experiments on THE4A

	Run no.					
	PC1-069	PC1-070	PC1-075	PC1-077	PC1-080	PC1-073
P (GPa)	1.0	1.2	1.4	1.5	1.6	1.7
n	4	6	6	6	5	8
SiO_2	71.48	71.53	71.07	71.91	74.37	72.86
TiO_2	0.36	0.30	0.34	0.28	0.19	0.27
Al_2O_3	16.38	16.25	16.01	16.27	16.64	16.32
FeO^T	1.99	1.26	1.64	1.49	1.27	1.10
MnO	0.04	0.06	0.03	0.06	0.09	0.09
MgO	1.08	0.66	0.90	0.66	0.42	0.45
CaO	2.84	2.32	2.78	2.51	2.38	2.29
Na_2O	4.21	5.92	5.61	5.17	3.07	4.97
K_2O	1.62	1.71	1.63	1.67	1.57	1.65
Mg#	49	48	49	44	37	42
K_2O/Na_2O	0.38	0.29	0.29	0.32	0.51	0.33
A/CNK	1.18	1.03	1.00	1.09	1.50	1.16
q	31.67	23.71	23.78	27.99	43.78	31.26
c	2.54	0.44		1.39	5.26	2.19
or	9.57	10.11	9.63	9.87	9.28	9.75
ab	36.19	50.09	47.47	43.75	25.98	42.05
an	13.52	11.51	13.69	12.45	11.81	11.36
di			0.08			
hy	5.82	3.57	4.71	4.03	3.23	2.86
il	0.68	0.57	0.65	0.53	0.36	0.51

[a] Normalised to 100% anhydrous, *n* = no. of analyses.

incoming of garnet, at 875 °C, is 1.45 GPa—very close to the pressure found experimentally.

Reaction products and their relative proportions vary with *P*, as shown in Fig. 11. The amount of melt produced was ≥75% for all runs and, as expected, melt compositions (Table 5) are generally trondhjemitic to granodioritic (Fig. 12). The high percentage of melt at 875 °C suggests that the TTG magmas were probably produced from their protoliths at temperatures around 900 °C, and very probably less than 1000 °C. Taking the inferred depth of origin into account, this implies that the TTG magmas were generated in a geothermal gradient <20 °C/km. Coexisting minerals are listed in Table 6. Typical near-liquidus ferromagnesian mineral assemblages were Hbl ± Cpx at $P \leq 1.5$ GPa and Hbl + Cpx + Grt at $P \geq 1.6$ GPa (all mineral abbreviations from Kretz, 1983). Plagioclase was not present in

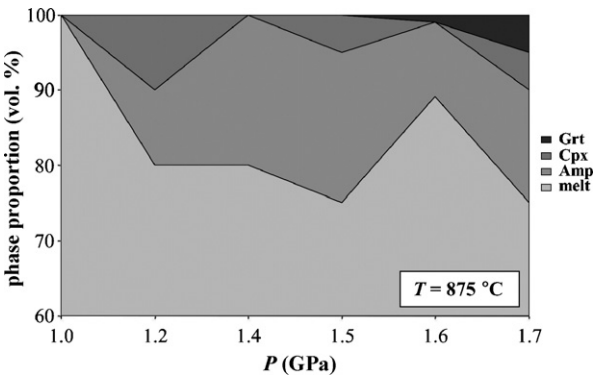

Fig. 11. Graph showing the proportions of phases in the products of near-liquidus experiments on THE4A. See text for further explanation.

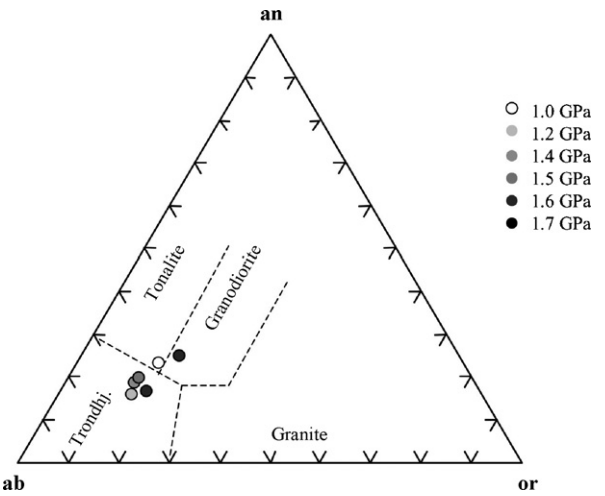

Fig. 12. Average glass (quenched melt) compositions produced in near-liquidus experiments on THE4A, at a range of pressures, plotted on the classification diagram of Barker (1979).

Table 6
Average major-element compositions[a] of minerals produced in near-liquidus experiments on THE4A

	Amp					Grt	Cpx		
P (GPa)	1.2	1.4	1.5	1.6	1.7	1.7	1.2	1.5	1.7
n	4	10	16	17	17	16	7	1	1
SiO_2	49.47	50.24	49.10	46.42	48.94	38.94	52.64	54.95	52.00
TiO_2	1.23	0.80	1.23	1.48	1.45	0.95	0.32	0.16	0.20
Al_2O_3	8.81	8.12	10.20	12.40	14.56	20.84	2.40	2.01	4.93
Cr_2O_3	0.09	0.17	0.08	0.11	0.06	0.11	0.12	0.12	–
Fe_2O_3	6.04	6.20	4.29	8.90	2.05	1.16	2.16	–	–
FeO	5.23	4.91	6.90	4.93	9.15	21.20	4.94	13.84	15.09
MnO	0.13	0.18	0.12	0.14	0.09	0.98	0.16	0.23	0.39
MgO	15.68	16.08	14.53	13.09	10.83	6.20	13.84	15.15	13.36
CaO	10.41	10.59	10.54	9.36	8.81	9.58	22.20	12.77	12.48
Na_2O	2.55	2.32	2.64	2.29	3.38	0.29	1.04	0.79	1.13
K_2O	0.35	0.39	0.38	0.82	0.66	0.08	0.07	0.01	0.41
xO^{2-}	23	23	23	23	23	12	6	6	6
Si	6.817	6.954	6.751	6.399	6.858	3.032	1.899	1.973	1.950
Ti	0.128	0.083	0.127	0.153	0.153	0.056	0.009	0.004	0.006
Al	1.431	1.323	1.652	2.017	2.406	1.911	0.102	0.085	0.218
Cr	0.010	0.019	0.009	0.011	0.007	0.007	0.003	0.003	–
Fe^{3+}	0.626	0.642	0.441	0.917	0.218	0.067	0.059	–	–
Fe^{2+}	0.604	0.574	0.795	0.575	1.075	1.380	0.148	0.416	0.473
Mn	0.016	0.021	0.014	0.016	0.011	0.065	0.005	0.007	0.012
Mg	3.220	3.316	2.977	2.688	2.268	0.719	0.744	0.811	0.747
Ca	1.536	1.572	1.552	1.385	1.327	0.799	0.858	0.491	0.502
Na	0.681	0.622	0.704	0.607	0.917	0.045	0.073	0.055	0.082
K	0.062	0.070	0.066	0.189	0.119	0.008	0.003	0.000	0.020
ΣCations	15.13	15.20	15.09	14.97	15.36	8.089	3.91	3.85	4.01
Mg#	84	85	79	82	68	34	83	66	61

[a] Normalised 100% anhydrous, Fe^{2+} and Fe^{3+} calculated using the method of Droop (1987).

the near-liquidus assemblages, confirming the interpretation based on the lack of a Eu anomaly, that feldspar was not present in the residuum. Textures in the run products are exemplified in the photomicrograph of the run product formed at 1.7 GPa (Fig. 13). Mineral compositions vary little with *P*. The amphiboles range from silicic edenite to magnesiohastingsitic hornblende, compared with the original edenitic hornblende in the starting material (THE4A). Garnet formed at 1.7 GPa has a composition of $Alm_{48}Prp_{24}Grs_{26}Sps_2$. Garnet formed at lower pressures was scarce, but easily identified in optical grain mounts, though it was not found during microprobe analysis. Pyroxenes are typically diopsidic at $P = 1.2$ GPa and augitic at $P \geq 1.5$ GPa. A very small amount of accessory rutile was identified in the products of the run at 1.7 GPa (Fig. 13), and may have been present in the other experiments, though it was not specifically identified. Residual rutile is required to explain the marked negative Nb, Ta and Ti anomalies shown by all TTG rocks (see, e.g. Fig. 5). The lack of plagioclase and presence of garnet and pyroxene in the near-liquidus assemblage suggest that the majority of TTGs coexisted with a hornblende-bearing eclogite rather than either an amphibolitic or granulitic residue.

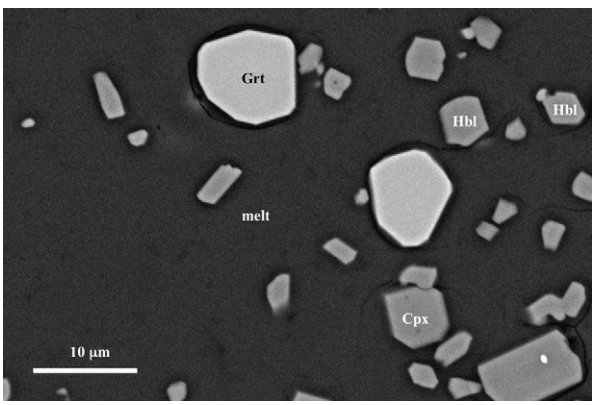

Fig. 13. Back-scattered electron photomicrograph of run PC1-073 (1.7 GPa) showing new garnet crystals in matrix glass (quenched melt).

5.2. Partial melting of Barberton amphibolite

In view of the results of the TTG near-liquidus experiments, the greenstone amphibolite experiments were all conducted at 1.6 GPa; results are shown in Table 4. Note

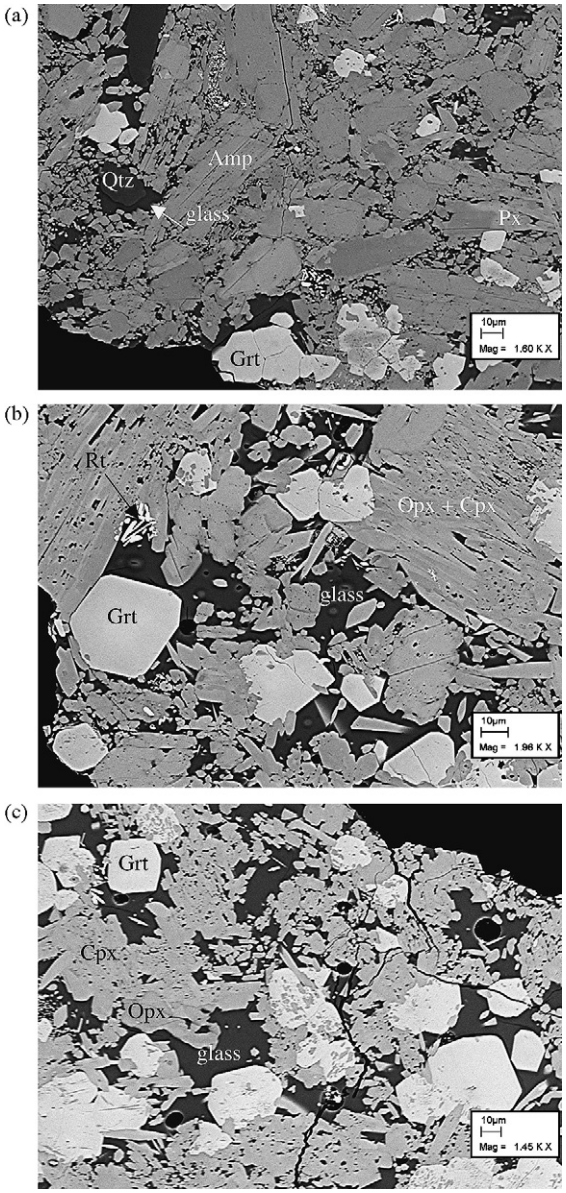

Fig. 14. Back-scattered electron photomicrographs showing the mineralogy and textures of the products of partial melting experiments (1.6 GPa) carried out on greenstone amphibolite AmX12-a, (a) at 875 °C, (b) at 925 °C and (c) at 1000 °C.

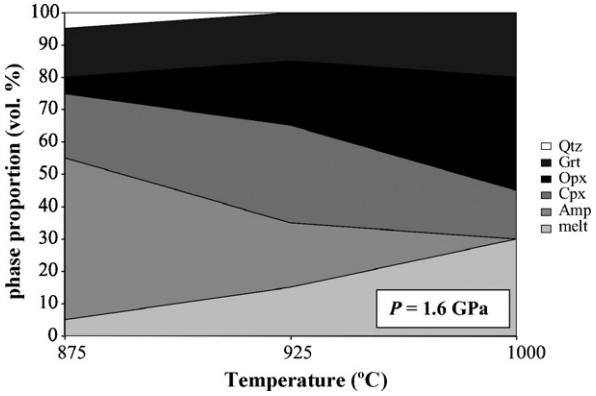

Fig. 15. Proportions of run products formed in the partial melting experiments on greenstone amphibolite AmX12-a.

that we have not attempted to determine the minimum pressure for appearance of garnet in this amphibolite, as this is not relevant to the problem being investigated. The pressure for the partial melting experiments was simply chosen as a suitable pressure, slightly above the necessary minimum, as determined from the near-liquidus experiments on the TTG (THE4A). Fig. 14 shows typical textures developed in the run products. Relative proportions of the phases in the run products are shown, as a function of *T*, in Fig. 15. The amount of melt increases with *T*, from ~5% at 875 °C to 30% at 1000 °C. Melt compositions are given in Table 7.

The compositions of coexisting minerals are given in Table 8. Full mineral assemblages are; Amp + Cpx + Opx + Grt + Qtz + Rt + Ap at 875 °C, Amp + Cpx + Opx + Grt + Rt + Ap at 925 °C and Cpx + Opx + Grt + Rt + Ap at 1000 °C (Fig. 14). The amphiboles are edenites to edenitic hornblendes, similar to those of the starting material. In the 875 °C run, large original hornblende crystals remain (Fig. 14a), indicating incomplete breakdown, due to the low degree of partial melting. Compositions of garnets are typically Alm-rich with Prp content increasing at higher *T* ($Alm_{46}Prp_{29}Grs_{22}Sps_3$ to $Alm_{38}Prp_{38}Grs_{23}Sps_1$) (Fig. 14b). Pyroxenes are typically augite, coexisting with enstatite, at all temperatures. Previous studies of fluid-absent partial melting of amphibolites, at about 1.5 GPa, produced pyroxenes with Jd contents, ranging from 8 to 14 mol.% with an average of 10 mol.% (Sen and Dunn, 1994; Rapp and Watson, 1995; Skjerlie and Patiño Douce, 2002). The Jd contents of the clinopyroxenes formed in the present work are 6–7.5 mol.%, similar to those formed in the near-liquidus runs on the TTG starting material. This difference is probably related to the bulk composition of the starting material and the particular phases coexisting with the clinopyroxenes. Experiments on a different amphibolitic starting material, carried out in the same apparatus, with the same experimental techniques, at 2 and 2.5 GPa (Xiao and Clemens, submitted for publication), produced strongly omphacitic pyroxenes coexisting with garnet and melt. In the present work, sodic hornblende was present, and at least as abundant as the coexisting clinopyroxene, up to about 920 °C (Fig. 15). Partitioning of Na between the amphibole and the pyroxene is probably a major control on the lower Jd contents of the

Table 7
Normalised 100% anhydrous analyses and CIPW norms of glasses (quenched melts) formed in fluid-absent partial melting experiments (1.6 GPa) on amphibolitised Barberton greenstone AmX12-a

	$T = 875\,^{\circ}C$, $n = 7$		$T = 925\,^{\circ}C$, $n = 11$		$T = 1000\,^{\circ}C$, $n = 5$	
	$\bar{X}$	σ	$\bar{X}$	σ	$\bar{X}$	σ
SiO_2	74.94	0.34	74.57	0.27	70.03	0.30
TiO_2	0.32	0.09	0.33	0.08	0.69	0.06
Al_2O_3	13.21	0.20	14.05	0.10	15.35	0.09
FeO^T	1.60	0.17	1.59	0.18	2.69	0.19
MgO	0.32	0.10	0.27	0.08	0.73	0.16
CaO	2.31	0.13	1.83	0.15	2.84	0.12
Na_2O	4.38	0.17	4.24	0.18	4.56	0.05
K_2O	2.90	0.12	3.10	0.13	3.12	0.13
K_2O/Na_2O	0.66		0.73		0.68	
A/CNK	0.91		1.02		0.96	

	$T = 875\,^{\circ}C$, $n = 7$	$T = 925\,^{\circ}C$, $n = 11$	$T = 1000\,^{\circ}C$, $n = 5$
q	35.64	32.65	23.06
or	17.14	18.32	18.44
ab	37.44	36.30	39.13
an	7.44	8.66	11.66
c	–	.39	–
di	3.12	–	1.60
hy	1.60	3.05	4.81
il	0.61	0.63	1.31
Mg#	26.3	23.2	32.6
An in plag.	16.6	19.3	23.0

FeO^T = total Fe as FeO; n = number of individual point analyses; $\bar{X}$ = sample mean; σ = standard deviation.

clinopyroxenes in the present work. In the products of the lower-T melting experiments, the two pyroxenes are quite complexly intergrown (see, e.g. Fig. 14b) while, at 1000 °C, the pyroxene crystals are more separated from each other (e.g. Fig. 14c). At 1.6 GPa, the quartz-out curve lies between 875 and 925 °C, and hornblende-out lies between 925 and 1000 °C.

5.3. Interpretation of melt compositions from amphibolite melting experiments

The main reaction for the partial melting of amphibolite under fluid-absent conditions, at pressures where garnet is stable is similar to:

$$\text{Hbl} + \text{Pl} = \text{Grt} + \text{Cpx} \pm \text{Opx} + \text{melt}.$$

The compositions of the glasses (quenched melts) (Table 7) are compared to the Barberton TTG rocks in Fig. 16. They are metaluminous or marginally peraluminous sodic granites, in many respects quite similar in composition to some of the more felsic TTG rocks. However, their compositions do not fall in the trondhjemite field (Fig. 16a), where the bulk of the Barberton TTGs plot.

Variations in melt composition with run T reflect the changes in stoichiometry of the incongruent melting reaction, as melting progresses. For example, SiO_2 contents of melts decrease, whereas the other oxides generally increase with increasing T. The reduction in SiO_2 and increase in CaO, FeO^T and TiO_2 reflect the increased degree of melting/dissolution of mafic phases as T increases. However, there is no progressive increase in CaO between 875 and 925 °C. This probably reflects the stability of clinopyroxene at these temperatures. Once T exceeds 925 °C, Cpx becomes unstable and then contributes Ca to the melt. Increases in Na_2O, with temperature, are typically ascribed to the melting of Na-rich minerals, the identity of which will change as a function of P and T. Plagioclase is not present in the residual assemblages at the conditions of our experiments, having been consumed in the above melting reaction by 875 °C. Increases in melt Na_2O content at higher T were therefore most probably the consequence of amphibole dissolution. Similarly, the trace of K-feldspar present in the starting material had disappeared by 875 °C. Despite this, higher temperature evolution to significantly larger melt volumes does not markedly shift the melt composition to less potassic (lower K_2O/Na_2O) compositions

Table 8
Average major-element compositions (normalised to 100%) of the minerals formed in fluid-absent partial melting experiments (1.6 GPa) on amphibolitised Barberton greenstone AmX12-a

Mineral	Amp		Grt			Cpx			Opx		
T (°C)	875	925	875	925	1000	875	925	1000	875	925	1000
n	6	1	6	5	5	1	4	3	2	3	5
SiO_2	47.25	47.44	38.41	38.67	39.71	53.22	52.04	51.04	54.75	52.38	52.58
TiO_2	0.88	1.07	0.94	1.13	1.42	0.33	0.43	0.57	0.20	0.24	0.46
Al_2O_3	11.78	9.59	20.72	20.69	21.22	3.38	5.09	5.24	6.00	3.71	3.14
Cr_2O_3	0.17	0.21	0.10	0.16	0.17	0.17	0.19	0.16	0.26	0.11	0.14
Fe_2O_3	5.61	2.00	1.85	1.86	1.23	–	0.22	0.59	–	0.32	0.54
FeO	7.86	11.55	20.96	19.69	17.81	10.19	9.40	9.81	18.52	19.08	18.74
MnO	0.26	0.10	1.23	0.65	0.61	0.24	0.13	0.17	0.38	0.33	0.24
MgO	12.86	13.57	7.59	8.83	9.80	13.51	13.25	13.47	16.48	22.31	22.99
CaO	10.92	12.39	8.00	8.15	8.11	17.75	18.30	18.21	2.30	1.31	1.33
Na_2O	1.79	1.50	0.14	0.15	0.19	0.97	1.08	0.89	0.76	0.32	0.19
K_2O	0.61	0.58	0.05	0.02	0.02	0.11	0.05	0.04	0.55	0.02	0.03
xO^{2-}	23	23	12	12	12	6	6	6	6	6	6
Si	6.522	6.628	5.604	5.687	5.934	1.839	1.856	1.823	1.996	1.883	1.859
Ti	0.092	0.113	0.103	0.125	0.159	0.008	0.012	0.015	0.005	0.006	0.012
Al	1.907	1.578	3.549	3.586	3.738	0.137	0.214	0.219	0.258	0.157	0.131
Cr	0.018	0.023	0.015	0.019	0.020	0.005	0.006	0.004	0.008	0.003	0.004
Fe^{3+}	0.574	0.211	0.159	0.206	0.140	–	0.006	0.016	–	0.009	0.015
Fe^{2+}	0.915	1.350	2.578	2.421	2.222	0.295	0.280	0.293	0.566	0.574	0.554
Mn	0.031	0.012	0.152	0.081	0.078	0.007	0.004	0.005	0.012	0.010	0.007
Mg	2.646	2.825	1.674	1.935	2.183	0.696	0.704	0.717	0.897	1.196	1.212
Ca	1.617	1.854	1.211	1.283	1.300	0.657	0.699	0.698	0.090	0.050	0.050
Na	0.478	0.405	0.037	0.042	0.055	0.065	0.075	0.061	0.054	0.023	0.014
K	0.108	0.104	0.009	0.004	0.004	0.005	0.002	0.002	0.026	0.001	0.001
Σ cations	14.91	15.10	16.00	15.39	15.80	3.71	3.85	3.85	3.91	3.91	3.85
Mg#	74	68	39	44	50	70	72	71	61	68	69

(see Table 7). This suggests gradual release of K during progressive hornblende breakdown.

In terms of residual mineralogy, the results of the partial melting experiments agree with both our near-liquidus experiments on the TTG (THE4A), and our interpretation of the trace-element and REE compositions of the TTG rocks. At the magma source, the TTG melts probably coexisted with sodic hornblende, augitic clinopyroxene and almandine-pyrope garnet, with a relatively high grossular content. Collectively, these data suggest that the TTGs were derived from a plagioclase-free garnet amphibolite or hornblende eclogite source, at a pressure of at least 1.5 GPa. The residual source probably contained around 20% hornblende. The experimentally observed garnet proportions (15–20%) are slightly too low to account for the observed HREE depletion in the TTGs, and the contribution for hornblende will be small. This confirms that 1.5 GPa is a minimum estimate for the pressure of melting.

The major-element compositions of the glasses match the natural rock compositions less well. In particular, the melt K_2O/Na_2O ratios (Table 7) are significantly higher and the Mg# lower than in most of the Barberton TTGs (Appendix A in supplementary data). The difference in Mg# probably reflects the relatively low melting proportion, even at 1000 °C, and the stability of Mg-rich restitic minerals in the solid residues. Given the observed behaviour of K_2O in the melting experiments, it is difficult to interpret this difference as related purely to melting conditions, although K_2O/Na_2O ratios of experimental melts, from a variety of source compositions, do increase with increasing P (Clemens et al., in press). Most probably, the high K_2O/Na_2O in the experimental melts reveals an important compositional difference between the Theespruit Formation amphibolite and the actual protolith for most of the Barberton TTGs. The absence of Opx from the near-liquidus assemblage of the experimental TTG contrasts with the presence of small amounts of this phase in the partial melting experiments on the Barberton amphibolite, a further indication that this sort of amphibolite is probably not the dominant source rock for the Barberton TTG magmas. Given that this composition appears to be representative of highest-grade metamafic rocks exposed in association with the

TTGs, this suggests the possibility that the TTG magmas were derived from a more sodic (lower K_2O/Na_2O) source that is not exposed among the high-grade metamorphic rocks of the Barberton greenstone belt.

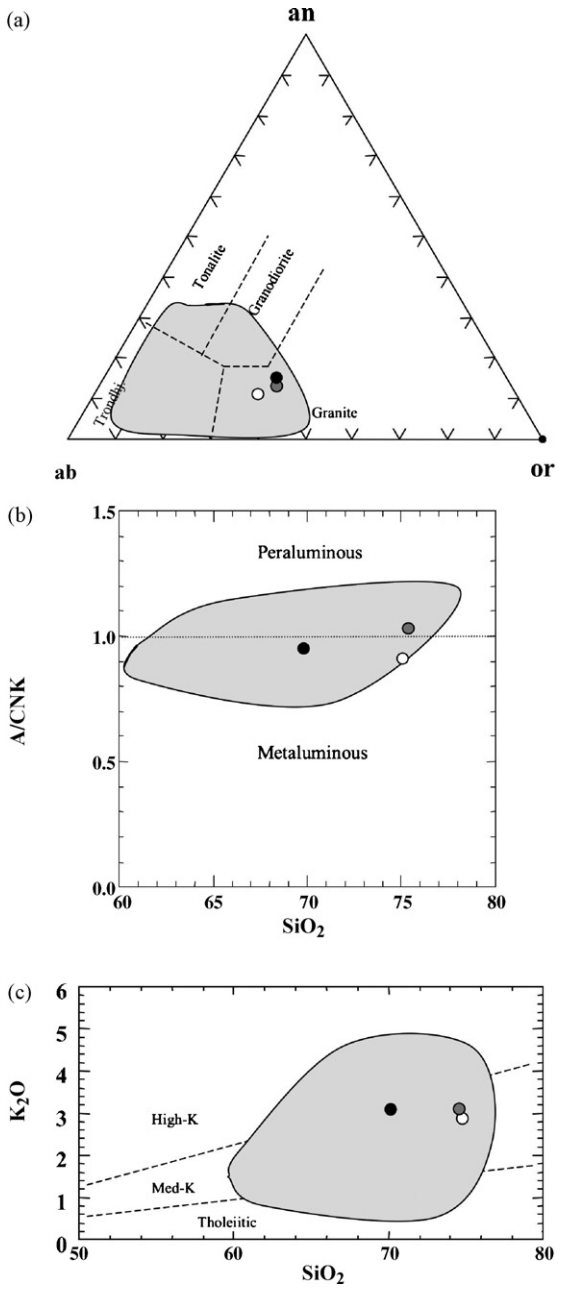

Fig. 16. (a–c) Diagrams showing the compositional fields occupied by the Barberton TTG rocks (light grey shading) and the compositions of the three glasses (quenched melts) produced in the partial melting experiments on greenstone amphibolite AmX12-a. White: 875 °C, mid grey: 925 °C and black: 1000 °C.

6. Discussion

Constraining the pressure at which near-liquidus garnet appears in the TTGs, to >1.47 GPa, is of considerable importance in the context of the Barberton Mountain Land. This confirms the general high pressures of magma derivation, implied by the REE geochemistry of the rocks, and demonstrates that the TTG magmas must have been produced at a depth of at least 50 km. This implies that the 3.45 Ga Archaean crust, represented by the southern portion of the Barberton granite-greenstone terrane, must have been at least this thick. In a modern tectonic scenario, this would constitute close to doubling of the thickness of typical continental crust. This is a phenomenon that, in the modern geological record, occurs only in tectonic settings that involve collision of terranes containing pre-existing continental crust. In the case of the ~3.23 Ga TTGs, this interpretation is consistent with the conclusions reached by several other workers who have focused on the style and age of deformation in the belt (de Ronde and De Wit, 1994; de Ronde and Kamo, 2000), sedimentary environments in the upper parts of the Barberton greenstone belt sequence (Lowe and Byerly, 1999), and the age and *P–T* conditions of the high-grade metamorphism (Dziggel et al., 2002). Thus, these magmas appear to have been coeval with a major terrane accretion event. This event is characterised by apparent geothermal gradients in the range of 18 °C/km (Dziggel et al., 2002; Kisters et al., 2003; Diener et al., 2005), as indicated by mineral assemblages in rocks exposed on the southern margin of the Belt and xenoliths in the ~3.45 Ga TTGs. This gradient is consistent with melting of thickened crust in the temperature range of 850–950 °C, at depths of 47–53 km.

Previous experiments have shown that TTG-like melts can be produced from metabasaltic protoliths at temperatures of 850–1000 °C (Rapp et al., 1991; Winther and Newton, 1991). Our partial melting experiments confirm that the rather more K-rich Barberton greenstones would produce sodic granite partial melts, but not trondhjemites—the dominant rock type among the Barberton TTG suite. Thus, it seems unlikely that the Barberton greenstones were the actual sources of the majority of the TTG magmas. The results imply that, at 3.45 and 3.23 Ga, less potassic (and probably older) mafic rocks must have underlain the Barberton terrane, and formed the source from which the TTG magmas were extracted. The pressure of formation of the Barberton TTG magmas (at least 1.47 GPa) suggests that geothermal gradients during TTG formation were of the same order at those during the metamorphism of the greenstones (around 18 °C/km; Dziggel et al., 2002; Kisters

et al., 2003). Thus, the findings of this study have a bearing on one of the central questions in Archaean geology, i.e. whether the mechanisms and rates of Archaean tectonics were fundamentally different to those that shaped younger orogenic belts (e.g. Hamilton, 1998; De Wit, 1998; Collins and Van Kranendonk, 1999).

The possibility that radiogenic heat production may have been significantly higher in the Archaean than at present (e.g. O'Nions et al., 1978; Davies, 1993) is central to this debate. Higher heat production may have produced circumstances detrimental to the development of lateral tectonics (Hargraves, 1986; Davies, 1992; Vlaar et al., 1994), favouring heat dissipation through mantle plumes (e.g. Campbell and Griffiths, 1992; Hill et al., 1992) rather than through linear magmatic spreading centres associated with lateral plate motions. Arndt et al. (1998) reviewed the data from various sources and argued that Mg-rich komatiite lavas in Archaean sequences (including Barberton) are dry melts of depleted mantle. This suggests very high magma temperatures, and an Archaean mantle much hotter than at present (e.g. Herzberg, 1995). However, the oldest TTG rocks documented in this study, which are characterised by HREE-depleted signatures, are the gneisses of the Stolzburg pluton, components of which have been dated at 3460 ± 5 Ma. Thus, melting in crust approximately 50 km thick occurred within 10–30 Myr of the time of komatiite volcanism in the lower Onverwacht. This close temporal association of high-pressure crustal melting and mantle melting supports the suggestion that all these magmas were produced in cratonic extensional basins, in arc-continent or intracontinental rifts (Kisters et al., 2003; Heubeck and Lowe, 1994; Lowe, 1994; Eriksson et al., 1994), associated with subduction zones. If this is correct, the komatiites may not represent abnormally high-T ultramafic magmas. Instead, liquidus depression by H_2O-rich fluid may have allowed partial melting of the relatively shallow mantle at only moderate temperatures (e.g. Parman et al., 1997; Grove and Parman, 2004). Thus, at this time, extensional environments seem to have been associated with crustal domains that had low apparent geothermal gradients in which hydrated crustal rocks underwent high-pressure metamorphism and partial melting. Such a setting is compatible with the occurrence of lateral tectonic processes at this early stage of Earth's crustal evolution.

7. Summary

Near-liquidus experiments on a Theespruit trondhjemite show that garnet is stable at $P \geq 1.47$ GPa. This suggests that the Barberton TTG magmas, with their characteristic HREE depletion, were generated at depths of at least 50 km. This inference is supported by previous experimental work on partial melting relations of tholeiitic amphibolites, and our own experiments on a Barberton greenstone amphibolite. Restites are likely to have been eclogitic, with mineral assemblages of $Cpx + Opx + Grt \pm Hbl \pm Qtz + Rt + Ap$. This study has important geodynamic implications. Firstly, the Archaean crust must have been thickened to at least 50 km in order to generate TTG magmas. This would explain why 3.23 Ga TTG magmatism is contemporaneous with episodes of terrane collision in the tectonic history of the Barberton region, and suggests a similar setting for the older TTGs, where the tectonic setting is uncertain. Secondly, the generation of TTG magmas must have produced a plagioclase-free eclogitic restite, in keeping with the REE geochemistry of the Barberton TTGs. Thirdly, the parent rocks for the bulk of the Barberton TTGs were not the Barberton greenstones but an older? mafic terrane that was structurally overlain by the Barberton.

Acknowledgement

This paper has benefited considerably from very detailed reviews by H. Martin and an anonymous reviewer.

Appendix A. Supplementary data

Supplementary data associated with this article can be found, in the online version, at doi:10.1016/j.precamres.2006.08.001.

References

Anhaeusser, C.R., Robb, L.J., 1983. Chemical analyses of granitoid rocks from the Barberton Mountain Land. Geol. Soc. S. Afr. Spec. Pub. 9, 189–223.

Armstrong, R.A., Compston, W., deWit, M.J., Williams, I.S., 1990. The stratigraphy of the Barberton greenstone belt revisited: a single zircon ion microprobe study. Earth Planet. Sci. Lett. 101, 90–106.

Arndt, N., et al., 1998. Were komatiites wet? Geology 26, 739–742.

Arth, J.G., Barker, F., Peterman, Z.E., Friedman, I., 1978. Geochemistry of the gabbro-diorite-tonalite-trondhjemite suite of southwest Finland and its implications for the origin of tonalitic and trondhjemitic magmas. J. Petrol. 19, 289–316.

Atherton, M.P., Petford, N., 1993. Generation of sodium-rich magmas from newly underplated basaltic crust. Nature 362, 144–146.

Barker, F., 1979. Trondhjemite: definition, environment and hypotheses of origin. In: Barker, F. (Ed.), Trondhjemites, Dacites and Related Rocks. Elsevier, Amsterdam, pp. 1–12.

Bea, F., 1996. Controls on the trace element composition of crustal melts. Transactions of the R. Soc. Edinburgh Earth Sciences 87, 33–41.

Campbell, I.H., Griffiths, R.W., 1992. The changing nature of mantle hotspots through time: implications for the chemical evolution of the mantle. J. Geol. 100, 497–523.

Chappell, B.W., White, A.J.R., 1974. Two contrasting granite types. Pac. Geol. 8, 173–174.

Clemens, J.D., 1984. Water contents of intermediate to silicic magmas. Lithos 17, 273–287.

Clemens, J.D., 2005. Melting of the continental crust: fluid regimes, melting reactions and source-rock fertility. In: Brown, M., Rushmer, T. (Eds.), Evolution and Differentiation of the Continental Crust. Cambridge University Press, pp. 297–331.

Clemens, J.D., Helps, P.A., Stevens, G. Chemical variations in granitic magmas: source-inherited or products of magmatic processes? Proc. R. Soc. Edinburgh, Earth Sci., in press.

Clemens, J.D., Vielzeuf, D., 1987. Constraints on melting and magma production in the crust. Earth Planet. Sci. Lett. 86, 287–306.

Clemens, J.D., Watkins, J.M., 2001. The fluid regime of high-temperature metamorphism during granitoid magma genesis. Contrib. Mineral. Petrol. 140, 600–606.

Collins, W.J., Van Kranendonk, M.J., 1999. Model for the development of kyanite during partial convective overturn of Archaean granite-greenstone terranes: the Pilbara Craton, Australia. J. Metamorphic Geol. 17, 145–156.

Condie, K.C., 2005. TTGs and adakites: are they both slab melts? Lithos 80, 33–44.

Connolly, J.A.D., 2005. Computation of phase equilibria by linear programming: a tool for geodynamic modeling and its application to subduction zone decarbonation. Earth Planet. Sci. Lett. 236, 524–541.

Davies, G.F., 1992. On the emergence of plate tectonics. Geology 20, 963–966.

Davies, G.F., 1993. Conjectures on the thermal and tectonic evolution of the earth. Lithos 30, 281–289.

de Ronde, C.E.J., De Wit, M.J., 1994. The tectonothermal evolution of the Barberton greenstone belt, South Africa: 490 million years of crustal evolution. Tectonics 13, 983–1005.

de Ronde, C.E.J., Kamo, S.L., 2000. An Archaean arc-arc collisional event: a short-lived, ca 3 Myr episode, Weltevreden area, Barberton greenstone belt, South Africa. J. Afr. Earth Sci. 30, 219–248.

De Wit, M.J., 1998. On Archaean granites, greenstones, cratons and tectonics: does the evidence demand a verdict? Precambrian Res. 91, 181–226.

De Wit, M.J., Armstrong, R.A., Hart, R.J., Wilson, A.H., 1987. Felsic igneous rocks within the 3.3–3.5 Ga Barberton greenstone belt: high-level equivalents of the surrounding tonalite trondhjemite terrain, emplaced during thrusting. Tectonics 6, 529–549.

Diener, J.F.A., Stevens, G., Kisters, A.F.M., Poujol, M., 2005. Geotectonic evolution of the Tjakastad Schist belt, Barberton greenstone belt, South Africa: A record of mid-Archaean metamorphism and terrain exhumation. Precambrian Res. 143, 87–112.

Diener J.F.A., 2004. The tectono-metamorphic evolution of the Theespruit Formation in the Tjakastad schist belt and surrounding areas of the Barberton greenstone belt, South Africa. M.Sc. Thesis (unpublished), Stellenbosch University, 208 pp.

Droop, G.T.R., 1987. A general equation for estimating Fe-3+ concentrations in ferromagnesian silicates and oxides from microprobe analyses, using stoichiometric criteria. Mineral. Mag. 51, 431–435.

Drummond, M.S., Defant, M.J., 1990. A model for trondhjemite-tonalite-dacite genesis and crustal growth via slab melting: archean to modern comparisons. J. Geophys. Res. Solid Earth 95, 21503–21521.

Dziggel, A., Stevens, G., Poujol, M., Anhaeusser, C.R., Armstrong, R.A., 2002. Metamorphism of the granite-greenstone terrane south of the Barberton greenstone belt, South Africa: and insight into the tectono-thermal evolution of the 'lower' portions of the Onverwacht Group. Precambrian Res. 114, 221–247.

Eriksson, K.A., Krapez, B., Fralick, P.W., 1994. Sedimentology of Archean greenstone belts—signatures of tectonic evolution. Earth Sci. Rev. 37, 1–88.

Foley, S., Tiepolo, M., Vannucci, R., 2002. Growth of early continental crust controlled by melting of amphibolite in subduction zones. Nature 417, 837–840.

Gao, S., Luo, T.-C., Zhang, B.-R., Zhang, H.-F., Han, Y.-W., Zhao, Z.-D., Hu, Y.-K., 1998. Chemical composition of the continental crust as revealed by studies in East China. Geochim. Cosmochim. Acta 62, 1959–11975.

Glazner, A.F., Bartley, J.M., Coleman, D.S., Gray, W., Taylor, R.Z., 2004. Are plutons assembled over millions of years by amalgamation from small magma chambers? GSA Today 14, 4–11.

Glikson, A.Y., 1979. Early Precambrian tonalite-trondhjemite sialic nuclei. Earth Sci. Rev. 15, 1–73.

Goldstein, S.L., O'Nions, R.K., Hamilton, P.J., 1984. A Sm-Nd isotopic study of atmospheric dusts and particulates from major river systems. Earth Planet. Sci. Lett. 70, 221–236.

Graphchikov, A.A., Konilov, A.N., Clemens, J.D., 1999. Biotite dehydration, partial melting, and fluid composition: experiments in the system $KAlO_2$–FeO–MgO–SiO_2–H_2O–CO_2. Am. Mineral. 84, 15–26.

Grove, T.L., Parman, S.W., 2004. Thermal evolution of the Earth as recorded by komatiites. Earth Planet. Sci. Lett. 219, 173–187.

Hamilton, W.B., 1998. Archaean magmatism and plate tectonics were not products of plate tectonics. Precambrian Res. 91, 143–179.

Hamilton, P.J., Evensen, N.M., O'Nions, R.K., 1979. Sm–Nd dating of Onverwacht Group volcanics, southern Africa. Nature 279, 298–300.

Hargraves, R.B., 1986. Faster spreading or greater ridge length in the Archaean. Geology 14, 750–752.

Haskin, L.A., Wildeman, T.R., Haskin, M.A., 1968. An accurate procedure for the determination of the rare earths by neutron activation. J. Radioanal. Chem. 1, 337–348.

Herzberg, C., 1995. Generation of plume magmas through time: an experimental perspective. Chem. Geol. 126, 1–16.

Heubeck, C., Lowe, D.R., 1994. Late syndepositional deformation and detachment tectonics in the Barberton Greenstone-Belt, South-Africa. Tectonics 13, 1514–1536.

Hill, R.I., Campbell, G.F., Davies, G.F., Griffiths, R.W., 1992. Mantle plumes and continental tectonics. Science 256, 186–193.

Jahn, B.M., Glikson, A.Y., Peucat, J.J., Hickman, A.H., 1981. REE geochemistry and isotopic data of Archaean silicic volcanics and granitoids from the Pilbara Block, Western Australia: implications for the early crustal evolution. Geochim. Cosmochim. Acta 45, 1633–1652.

Jahn, B.M., Vidal, P., Kröner, A., 1984. Multichronometric ages and origin of Archaean tonalitic gneisses in Finnish Lapland: a case for long crustal residence time. Contrib. Mineral. Petrol. 86, 398–408.

Johnston, A.D., Wyllie, P.J., 1988. Constraints on the origin of Archean trondhjemites based on phase relationships of Nûk gneiss with H_2O at 15 kbar. Contrib. Mineral. Petrol. 100, 35–46.

Kamo, S.L., Davis, D.W., 1994. Reassessment of Archaean crustal development in the Barberton Mountain Land, South Africa, based on U-Pb dating. Tectonics 13, 167–192.

Kisters, A.F.M., Stevens, G., Dziggel, A., Armstrong, R.A., 2003. Extensional detachment faulting and core-complex formation in the southern Barberton granite-greenstone terrain, South Africa: evidence for a 3.2 Ga orogenic collapse. Precambrian Res. 127, 355–378.

Kretz, R., 1983. Symbols for rock-forming minerals. Am. Mineral. 68, 277–279.

Kröner, A., Byerly, G.R., Lowe, D.R., 1991. Chronology of early Archaean granite-greenstone evolution in the Barberton Mountainland, South Africa, based on precise dating by single zircon evaporation. Earth Planet. Sci. Lett. 103, 41–54.

Kröner, A., Hegner, E., Wendt, J.I., Byerly, G.R., 1996. The oldest part of the Barberton granitoid-greenstone terrain, South Africa, evidence for crust formation between 3.5 and 3.7 Ga. Precambrian Res. 78, 105–124.

Le Maitre, R.W., Bateman, P., Dudek, A., Keller, J., Lameyre Le Bas, M.J., Sabine, P.A., Schmid, R., Sorensen, H., Streckeisen, A., Woolley, A.R., Zanettin, B., 1989. A Classification of Igneous Rocks and Glossary of Terms. Blackwell, Oxford, 193 pp.

Lowe, D.R., 1994. Accretionary history of the Archean Barberton Greenstone-Belt (3.55–3.22 Ga), Southern Africa. Geology 22, 1099–1102.

Lowe, D.R., Byerly, G.R., 1999. Stratigraphy of the west-central part of the Barberton Greenstone Belt, South Africa. Geol. Soc. Am. Spec. Pap. 329, 1–36.

Martin, H., 1986. Effect of steeper Archaean geothermal gradient on geochemistry of subduction-zone magmas. Geology 14, 753–756.

Martin, H., 1987. Petrogenesis of Archaean trondhjemites, tonalites and granodiorites from Eastern Finland: major and trace element geochemistry. J. Petrol. 28, 921–953.

Martin, H., 1994. The Archean grey gneisses and the genesis of the continental crust. In: Condie, K.C. (Ed.), Archean Crustal Evolution. Elsevier, Amsterdam, pp. 205–259.

Martin, H., Moyen, J.F., 2002. Secular changes in tonalite-trondhjemite-granodiorite composition as markers of the progressive cooling of Earth. Geology 30, 319–322.

Martin, H., Smithies, R.H., Rapp, R., Moyen, J.F., Champion, D., 2005. An overview of adakite, tonalite-trondhjemite-granodiorite (TTG), and sanukitoid: relationships and some implications for crustal evolution. Lithos 79, 1–24.

McDonough, W.F., Sun, S.-S., 1995. Composition of the Earth. Chem. Geol. 120, 223–253.

Moorbath, S., 1975. Evolution of Precambrian crust from strontium evidence. Nature 254, 395–398.

Moyen, J.-F., Stevens, G., 2005. Experimental constraints on TTG petrogenesis: implications for Archean geodynamics. In: Benn, K., Mareschal, J.-C., Condie, K.C. (Eds.), Archean Geodynamics and Environments, Geophysical Monograph Series 164, pp. 149–175.

Nakamura, N., 1974. Determination of REE, Ba, Fe, Mg, Na, and K in carbonaceous and ordinary chondrites. Geochim. Cosmochim. Acta 38, 757–775.

O'Nions, R.K., Evensen, N.M., Hamilton, P.J., Carter, S.R., 1978. Melting of the mantle past and present: isotopic trace element evidence. Phil. Trans. R. Soc. Lond. A258, 547–559.

Parman, S.W., Dann, J.C., Grove, T.L., De Wit, M.J., 1997. Emplacement conditions of komatiite magmas from the 3.49 Ga Komati Formation, Barberton Greenstone Belt, South Africa. Earth Planet. Sci. Lett. 150, 303–323.

Petford, N., Atherton, M., 1996. Na-rich partial melts from newly underplated basaltic crust: the Cordillera Blanca Batholith, Peru. J. Petrol. 37, 1491–1521.

Prouteau, G., Maury, R.C., Scaillet, B., Pichavant, M., 1999. Fluid-present melting of ocean crust in subduction zones. Geology 27, 1111–1114.

Prouteau, G., Scaillet, B., Pichavant, M., Maury, R., 2001. Evidence for mantle metasomatism by hydrous silicic melts derived from subducted oceanic crust. Nature 410, 197–200.

Rapp, R.P., Shimizu, N., Norman, M.D., Applegate, G.S., 1999. Reaction between slab-derived melts and peridotite in the mantle wedge: experimental constraints at 3.8 GPa. Chem. Geol. 160, 335–356.

Rapp, R.P., Shimizu, N., Norman, M.D., 2003. Growth of early continental crust by partial melting of eclogite. Nature 425, 605–608.

Rapp, R.P., Watson, E.B., 1995. Dehydration melting of metabasalt at 8–32 kbar: implications for continental growth and crust-mantle recycling. J. Petrol. 36, 891–931.

Rapp, R.P., Watson, E.B., Miller, C.F., 1991. Partial melting of amphibolite/eclogite and the origin of Archean trondhjemites and tholeiites. Precambrian Res. 51, 1–25.

Robb, L.J., 1983. The nature, origin and significance of Archaean migmatites in the Barberton Mountain Land: a new approach in the assessment of early crustal evolution. Geol. Soc. S. Afr. Spec. Pub. 9, 81–101.

Robb, L.J., Anhaeusser, C.R., 1983. Chemical and petrogenetic characteristics of Archaean tonalite-trondhjemite gneiss plutons in the Barberton Mountain Land. Geol. Soc. S. Afr. Spec. Pub. 9, 103–117.

Rollinson, H.R., 1993. Using Geochemical Data: Evaluation, Presentation, Interpretation. Longman Scientific & Technical, London, pp. 352.

Scaillet, B., Holtz, F., Pichavant, M., 1998. Phase equilibrium constraints on the viscosity of silicic magmas—1. Volcanic-plutonic association. J. Geophys. Res. Solid Earth 103, 27257–27266.

Sen, C., Dunn, T., 1994. Dehydration melting of a basaltic composition amphibolite at 1.5 and 2.0 GPa: implications for the origin of adakites. Contrib. Mineral. Petrol. 117, 394–409.

Skjerlie, K.P., Patiño Douce, A.E., 2002. The fluid-absent partial melting of a zoisite-bearing quartz eclogite from 1.0 to 3.2 GPa; implications for melting in thickened continental crust and for subduction-zone processes. J. Petrol. 43, 291–314.

Smithies, R.H., 2000. The Archaean tonalite-trondhjemite-granodiorite (TTG) series is not an analogue of Cenozoic adakite. Earth Planet. Sci. Lett. 182, 115–125.

Springer, W., Seck, H.A., 1997. Partial fusion of basic granulites at 5 to 15 kbar: implications for the origin of TTG magmas. Contrib. Mineral. Petrol. 127, 30–45.

Stevens, G., Clemens, J.D., 1993. Fluid-absent melting and the roles of fluids in the lithosphere: a slanted summary? Chem. Geol. 108, 1–17.

Vielzeuf, D., Clemens, J.D., 1992. Fluid-absent melting of phlogopite + quartz: experiments and models. Am. Mineral. 77, 1206–1222.

Viljoen, M.J., Viljoen, R.P., 1969. An introduction to the Geology of the Barberton granite-greenstone terrain. Geol. Soc. South Africa Spec. Pub. 2, 9–28.

Vlaar, N.J., van Keken, P.E., van den Berg, A.P., 1994. Cooling of the Earth in the Archaean: consequences of pressure release melting in a hotter mantle. Earth Planet. Sci. Lett. 121, 1–18.

Wells, P.R.A., 1981. Accretion of continental crust: thermal and geochemical consequences. Phil. Trans. R. Soc. Lond. A301, 347–357.

Winther, K.T., 1996. An experimentally based model for the origin of tonalitic and trondhjemitic melts. Chem. Geol. 127, 43–59.

Winther, K.T., Newton, R.C., 1991. Experimental melting of hydrous low-K tholeiite: evidence on the origin of Archaean cratons. Bull. Geol. Soc. Denmark 39, 213–228.

Wyborn, D., Chappell, B.W., James, M., 2001. Examples of convective fractionation in high-temperature granites from the Lachlan Fold Belt. Aust. J. Earth Sci. 48, 531–541.

Xiao, L., Clemens, J.D., 2006. Origin of potassic (C-type) adakite magmas: experimental and field constraints. Lithos, submitted for publication.

Xu, J.F., Shinjo, R., Defant, M.J., Wang, Q.A., Rapp, R.P., 2002. Origin of Mesozoic adakitic intrusive rocks in the Ningzhen area of east China: partial melting of delaminated lower continental crust? Geology 30, 1111–1114.